Forest Ecosystems 10 (2023) 100150

Contents lists available at ScienceDirect

Forest Ecosystems

journal homepage: www.keaipublishing.com/cn/journals/forest-ecosystems

Silver fir tree-ring fluctuations decrease from north to south latitude—total solar irradiance and NAO are indicated as the main influencing factors

Václav Šimůnek[a,*], Anna Prokůpková[a], Zdeněk Vacek[a], Stanislav Vacek[a], Jan Cukor[a,b], Jiří Remeš[a], Vojtěch Hájek[a], Giuseppe D'Andrea[a], Martin Šálek[b,c,g], Paola Nola[d], Osvaldo Pericolo[d], Šárka Holzbachová[e], Francesco Ripullone[f]

[a] Faculty of Forestry and Wood Sciences, Czech University of Life Sciences Prague, Kamýcká 129, CZ—165 00, Prague 6, Suchdol, Czech Republic
[b] Forestry and Game Management Research Institute, v.v.i, Strnady 136, 252 02, Jíloviště, Czech Republic
[c] Czech Academy of Sciences, Institute of Vertebrate Biology, Květná 8, 603 65, Brno, Czech Republic
[d] Department of Earth and Environmental Sciences, University of Pavia, Via S. Epifanio 14, I-27100, Pavia, Italy
[e] Forests of the Czech Republic, SOE, Přemyslova 1106/19, Nový Hradec Králové, 500 08, Hradec Králové, Czech Republic
[f] School of Agricultural, Forestry and Environmental Sciences, University of Basilicata, Viale dell'Ateneo Lucano 10, I-85100, Potenza, Italy
[g] Faculty of Environmental Sciences, Czech University of Life Sciences Prague, Kamýcká 129, CZ—165 00, Prague, Suchdol, Czech Republic

ARTICLE INFO

Keywords:
Abies alba Mill.
Tree-rings
Solar cycle
North Atlantic oscillation
Precipitation
Temperature

ABSTRACT

Silver fir (*Abies alba* Mill.) is a flexible European tree species, mainly vegetating within the mountainous regions of Europe, but its growth responses across its latitudinal and longitudinal range have not yet been satisfactorily verified under changing environmental conditions. This study describes the tree-ring increment of silver fir in research plots across a latitudinal gradient from the northern range in Czechia (CZ), through Croatia (HR) to the southernmost range in Italy (IT). The research aims to analyze in detail the dynamics and cyclicity of the ring-width index (RWI) and how it relates to climatic factors (temperature and precipitation), the North Atlantic Oscillation (NAO), and total solar irradiance (TSI), including the determination of latitude. The results show that the main drivers affecting fir growth are the seasonal NAO index and TSI. Monthly temperatures affect RWI early in the vegetation season, while lack of precipitation during the summer is a limiting factor for fir growth, especially in July. Seasonal temperatures and temperatures in June and July negatively impact, while seasonal precipitation totals in the same months positively influence the RWI in all research plots across meridian. The longest growth cycles in fir RWI were recorded in the northernmost studied plots in CZ. These cyclical fluctuations recede approaching the south. The cyclic increase in RWI is related to the TSI, which decreases its effect from north to south. The TSI's effects vary, positively impacting CZ but negatively influencing HR while remaining relatively neutral in IT. On the other hand, seasonal NAO tends to negatively affect silver fir growth in HR and CZ but has a mildly positive effect in IT. In conclusion, the TSI and the influence of the seasonal NAO index are prevalent in the fir RWI and are accompanied by a greater cyclicity of RWI in Central Europe (temperature optimum) than in the Italian Mediterranean region, where this tree species is limited by climatic conditions, especially lack of precipitation.

1. Introduction

The natural distribution of silver fir (*Abies alba* Mill.) is in Central and Southern Europe, with the core areas of its distribution located in areas with relatively high precipitation during the growing season (Konnert and Bergmann, 1995; Volařík and Hédl, 2013; Gazol et al., 2015). The silver fir distribution in the Mediterranean area is limited by climate change, where the tree species is retreating to higher mountainous areas during the recent years. Due to increase in average temperatures, climate change allows for the expansion of this tree species to North-Eastern Europe, provided that precipitation is sufficient (Anić et al., 2009; Ruosch et al., 2016; Vitasse et al., 2019). Currently, fir is experiencing an increase in economic importance, making it an alternative to spruce in the restoration of monocultures in Central Europe during climate change (Vacek et al., 2023; Bosela et al., 2019; Mikulenka et al., 2020). At lower latitudes, fir distribution is limited mainly by insufficient precipitation

* Corresponding author.
E-mail address: simunekv@fld.czu.cz (V. Šimůnek).

https://doi.org/10.1016/j.fecs.2023.100150
Received 24 July 2023; Received in revised form 15 November 2023; Accepted 15 November 2023

(Pinto et al., 2008; Podrázský et al., 2018), which can be compensated by higher soil water content and abundant atmospheric moisture in valleys or localities with adequate ground moisture (Vitasse et al., 2019). However, fir does not tolerate permanently waterlogged habitats (Kučeravá et al., 2013). The other aspects determining its northern limit of distribution and growth in mountainous areas are low temperatures and spring frosts (Maxime and Hendrik, 2011; Gazol et al., 2019).

Silver fir expands to new habitats much slower than European beech (*Fagus sylvatica* L.) (Magri, 2008) or Norway spruce (*Picea abies* (L.) Karst.) (Caudullo et al., 2016; Tinner and Lotter, 2006). It is tolerant to shading and can grow at an older age after the canopy opens (Kučeravá et al., 2013). Compared to beech, it tolerates frosts better but not droughts (Maxime and Hendrik, 2011). The expansion of fir was previously limited by the impact of the air pollution calamity in the late 20th century when acid rain reduced fir stands in mountainous areas in Central Europe (Vacek et al., 2023; Kolář et al., 2015; Mikulenka et al., 2020). Ultimately, the natural regeneration of fir is strongly limited by wildlife-induced damage (Volařík and Hédl, 2013; Slanař et al., 2017; Vacek, 2017).

Climate change negatively affects the growth of forest tree species, the so-called divergence between drought and precipitation distribution in Europe (Stagge et al., 2017; Vacek et al., 2023). Among other things, this is caused by rising air temperatures, which are also reflected in more frequent and longer dry periods (Saffioti et al., 2016; Kelebek et al., 2021; Ossó et al., 2022). The climate of Europe is significantly influenced by the North Atlantic Oscillation (NAO) and divergent wind patterns, but these vary with climate change and may affect climatic conditions differently along latitudinal gradients. In particular, the NAO at the beginning of the vegetation season slightly influences temperatures of the summer (Kjellström et al., 2013).

The NAO has been linked to both precipitation and the influence of the airflow on dry seasons (Tsanis and Tapoglou, 2019). Precipitation totals in Central and Southern Europe are significantly influenced by NAO and are also significantly related to the solar cycle (Laurenz et al., 2019). Solar cycles influence European temperatures and indirectly affect NAO as well (Bice et al., 2012). The sunspot number cycle is associated with the cloud formation (and properties) in the atmosphere, which is also caused by cosmic ray ionization, and thus indirectly related to the cooling or warming of the planet (Jayaraman et al., 1998; Haywood and Boucher, 2000; Maghrabi and Kudela, 2019). The solar cycle can also affect jet streams, making them either direct or blocked, resulting in irregularities in the NAO over the solar cycle (Hall et al., 2015; Ma et al., 2018).

The circulation of NAO is determined by a positive or negative phase. A negative phase can bring cooler weather with less precipitation to Central Europe and warmer weather with more precipitation to the Mediterranean region. Conversely, the positive phase of NAO can cause warmer wet weather in Central Europe and cooler dry weather in the Mediterranean (Vicente-Serrano et al., 2011; Yao and Luo, 2014; Steirou et al., 2017; Tatli and Menteş, 2019).

Recently, there has been a continuous increase in air temperature in the northern hemisphere which is dissipated by the NAO flow, especially in winter and pre-spring. Conversely, in summer and autumn, the impact of NAO on temperature evolution is less prominent (Iles and Hegerl, 2017). When NAO is blocked, significant frost often occurs during the winter period, and conversely, high temperature extremes develop during a positive NAO (Diao et al., 2015). However, overall, NAO appears to influence the pattern of precipitation more than temperature (Kjellström et al., 2013; Lüdecke et al., 2020).

The influence of the NAO and the solar cycle is also reflected in the annual growth of trees. Across Europe, there may be different responses between NAO and tree-ring analyses, but the relationship is not spatially regular and is often associated with other indirect effects of local climate and seasonal tree growth (St. George, 2014). However, NAO can have a considerable indirect influence on tree-ring increment, primarily during February, when precipitation can affect future groundwater levels at the site (Akhmetzyanov et al., 2023). For example, European beech tree-ring increment in central Italy shows minimal variation and association with NAO (Piovesan et al., 2008). In Central Europe, however, there have been changes in tree-ring increment responses to the NAO over the last century, with the 20th century showing different trends than the 19th century (St. George, 2014). The circulation of NAO is immediately affected, but also up to three years in the solar cycle retroactively, causing jet streams to be blocked again (Gray et al., 2016). Therefore, the solar cycle may also be reflected in the tree-ring growth in Europe. It appears, for example, in tree rings in Russia (Shumilov et al., 2011; Kasatkina et al., 2019), Portugal (Dorotovič et al., 2014), Bulgaria (Komitov, 2021), or even Central and Southern Europe (Surový et al., 2008; Šimůnek et al., 2021b).

The total solar irradiance (TSI) represents the amount of solar energy received at the top of the Earth's atmosphere (Lean et al., 2005). The sunspot cycle manifests in the TSI, which causes the oscillation deviations with solar cycle (Lean et al., 1995; Kopp et al., 2016). For the global surface temperature anomaly, the TSI and cloud covers have played a significant role (Singh and Bhargawa, 2020). The TSI is a part of the influence from the solar cycle and solar forcing from Top-down (theory working on direct solar radiation and UV influence) and Bottom-up mechanisms (indirect solar effect on the air circulation mechanisms), while these kinds of forcing do not amplify direct forcing by a large amount.

Two primary theories, the Top-down and Bottom-up mechanisms, attempt to explain how solar cycles affect climate patterns. The Top-down mechanism emphasizes the role of solar radiation, particularly total solar irradiance (TSI), in directly impacting atmospheric processes. The variability in TSI influences the Earth's energy budget, affecting temperature and weather patterns. Numerous studies have explored the relationship between TSI and climate parameters (Wang et al., 2005; Gray et al., 2010).

On the other hand, the Bottom-up mechanism focuses on the indirect influence of solar activity on climate through modulating atmospheric circulation patterns. The NAO is a key component in this theory, representing the fluctuations in atmospheric pressure over the North Atlantic region. NAO phases, as highlighted in works, are associated with distinct climate patterns in Europe (Hurrell, 1995; Jones et al., 1997). Solar-induced changes in atmospheric circulation, as proposed by the Bottom-up mechanism, can impact regional climates and subsequently influence tree growth, as observed in dendrochronological studies (Esper et al., 2002; Büntgen et al., 2012).

The interplay between TSI, NAO, and the solar cycle is complex and interconnected. TSI acts as a direct driver in the Top-down mechanism, influencing temperature and weather, while NAO, in the Bottom-up mechanism, reflects the solar-induced changes in atmospheric circulation that contribute to regional climate variations.

The influence of the NAO and the TSI in relation to the solar cycle has not been considered in the most recent scientific works regarding the analysis of tree-ring increment in the Central European region in context to southern European region. Therefore, the main objective of this paper is to describe the factors influencing the tree-ring growth of silver fir in a geographical gradient of sites lying on the 16th meridian from Central Europe to the south of the Apennine Peninsula. The study evaluates the period from 1990 to 2021, in which the most intense changes in air temperatures occurred, creating divergence in the sensitivity of the tree-ring data to climate (St. George, 2014) and in the response of tree species to altitude to warmer air temperatures (Di Filippo et al., 2007; Tumajer et al., 2017), while this time period also excludes the effect of the air pollution effect in the Czech republic sites (Kolář et al., 2015; Putalová et al., 2019; Mikulenka et al., 2020). The aims of this study are (i) to determine the influence of climatic factors (temperature and precipitation), NAO, and TSI on the tree-ring growth of silver fir across the geographical latitudinal gradient of distribution and (ii) to analyze the cyclical characteristics and fluctuations of the tree-ring increment of silver fir from Central to Southern Europe.

2. Methods

2.1. Study area

The study area is located across the European distribution of silver fir—from Czechia (CZ) in the north, through Croatia (HR) to the southern edge of the distribution in Italy (IT) (Fig. 1). Research plots were established in mountainous areas (660–1,334 m a.s.l.) with natural presence of silver fir with a mean age of 60–74 years, with admixed Norway spruce and European beech. The research plots are located near the 16th meridian focusing on the occurrence of fir in those forest environments. Three mountain ranges were selected for the study, with three research sites chosen in each mountain range to capture the growth variability in the areas studied. In Czechia, the northernmost study sites are located in the Hrubý Jeseník Mountains. In Croatia, the Medvednica Mountains, which is in the middle of its natural range, and in Italy, the plots are located in the Lucanian Apennines in the southernmost part of the firs' range (see Table 1). Typologically, the communities belong to the association *Luzulo-Abiete-tum albae* and *Vaccinio vitis-idaeae-Abietetum albae* Oberdorfer 1957.

The precipitation and temperature conditions are different for each of the states, characterized by the meteorological station. Detailed climatic conditions of the research plots are described in Table 2. In Czechia, the research plots, according to the Köppen classification, are located in the Dfb humid continental climate, characterized by hot summers and cold winters. In Croatia, the research plots are in the Cfa humid subtropical climate, characterized by humid summers and cool to mild winters. Italian research plots are located in Csb, a warm-summer Mediterranean climate characterized by a dry-summer climate (Köppen, 1936). The duration of the growing season spans from 120 to 140 days.

2.2. Data collection

For dendrochronological analysis of the samples, silver fir increment cores were obtained using the Pressler auger (Haglöf, Långsele, Västernorrland, Sweden) at a height of 1.3 m above the ground, perpendicular to the trunk axis. Structurally homogeneous fir stands with a full stem density were selected for sampling. Samples were collected in 50 m × 50 m research plots from randomly selected (RNG function, Excel) healthy dominant and co-dominant trees according to the Kraft classification (Kraft, 1884), as the significant growth response (compared to sub-dominant and suppressed trees, Remeš et al., 2015). The average diameter of the evaluated trees at breast height was at least DBH > 20 cm. All tree heights on the research plots were measured with a Laser Vertex hypsometer (Haglöf, Långsele, Västernorrland, Sweden) with an accuracy of 0.1 m. The DBH of all trees was measured using a Mantax Blue metal caliper (Haglöf, Långsele, Västernorrland, Sweden) with tool accuracy of 1 mm. A total of 315 dendrochronological samples were

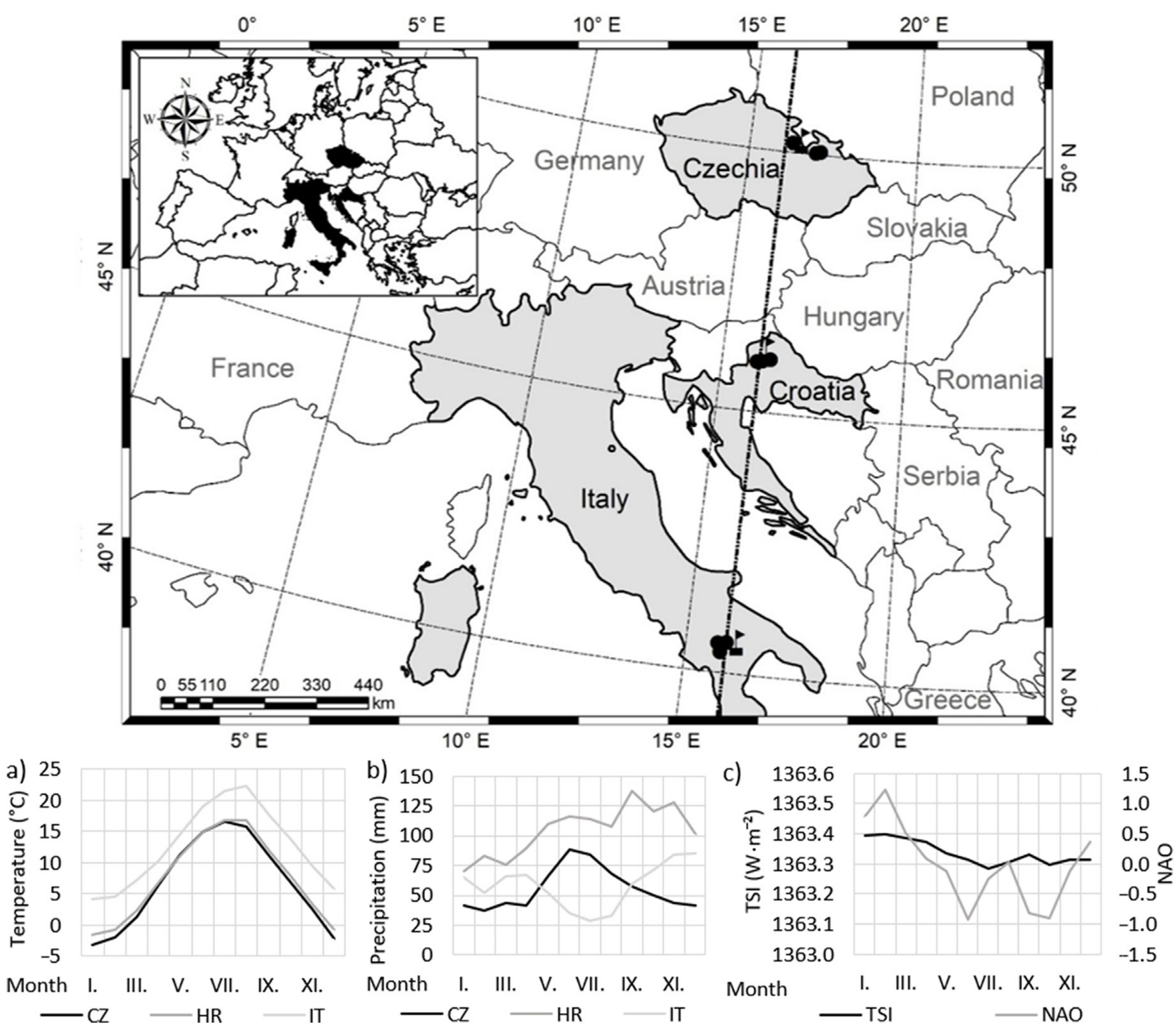

Fig. 1. Location of research plots (upper figure) in Czechia, Croatia, and Italy with the meteorological stations used for dendrochronological analyses (black flags) with the 16-meridian highlighted. Meteorological and data indicators (down part) used in the research describes average monthly average value in calendar year in 1990–2021: **(a)** monthly temperature; **(b)** monthly precipitation; **(c)** monthly TSI number and NAO.

Table 1
Basic site and stand characteristics of silver fir research plots.

Plot name	Location	Altitude (m a.s.l.)	Exposure	Slope (%)	Mean (m)	Mean (cm)	Volume ($m^3·ha^{-1}$)	Soil type	Climate class
CZ_1	50°22′40″N 16°21′41″E	790	S	10	21.2	25.8	346	Cambisols	Dfb
CZ_2	49°56′34″N 17°13′49″E	660	SE	3	23.6	31.8	387	Gleysol	Dfb
CZ_3	49°56′36″N 17°13′47″E	670	SE	3	22.1	28.9	398	Gleysol	Dfb
HR_1	45°54′30″N 15°58′33″E	923	E	4	19.4	28.4	246	Cambisols	Cfa
HR_2	45°54′17″N 15°58′09″E	978	SE	2	22.6	32.2	361	Cambisols	Cfa
HR_3	45°55′03″N 15°58′49″E	876	SE	2	21.4	28.7	227	Cambisols	Cfa
IT_1	40°42′03″N 15°43′50″E	944	NW	10	18.7	23.0	220	Cambisols	Csb
IT_2	40°30′42″N 15°46′01″E	1,324	NE	9	21.8	27.4	288	Cambisols	Csb
IT_3	40°24′09″N 15°56′57″E	1,158	N	9	25.4	28.1	289	Cambisols	Csb

Notes: climate classification according to Köppen (1936): Cfa—humid subtropical climate, Csb—Warm-summer Mediterranean climate, Dfb—warm-summer humid continental climate.

Table 2
Basic site stand characteristics of silver fir plots.

Plot	Met. station name	GPS of met. station	Station altitude (m a.s.l.)	Distance to plot (km)	Seasonal period (range)	Annual temp. (°C)	Seasonal temp. (°C)	Annual prec. (mm)	Seasonal prec. (mm)
CZ_1	Světlá Hora	50°02′46″N	593	82.3	May–September	6.6	13.9	661	363
CZ_2		17°23′50″E		15.5					
CZ_3				15.3					
HR_1	Puntijarka	45°54′28.8″N	988	0.6	May–September	7.4	14.3	1255	585
HR_2		15°58′04.8″E		0.2					
HR_3				1.5					
IT_1	Potenza	40°37′47.9″N	720	9.8	May–September	12.5	18.9	695	209
IT_2		15°48′00.2″E		13.4					
IT_3				28.3					

Notes: Met.—meteorological; Temp.—mean year air temperature; Prec.—annual precipitation.

collected, out of which 289 samples were selected for further dendrochronological analyses.

Tree-ring width was measured on all the increment cores using a LINTAB measuring table equipped with an Olympus microscope. The measuring table has a precision of 0.01 mm, and the TSAP-Win software was utilized to record the chronologies of each tree-ring width. (Rinntech, 2010). Subsequent cross-dating of the measured tree-ring cores was carried out using Cdendro software (Cybis Elektronik & Data AB, Sweden). The cross-correlation index (CC) for measured tree-ring sample was greater than C > 25 compared to the other samples (Larsson, 2013).

Monthly air temperature and precipitation data for Czechia were obtained from the Czech Hydrometeorological Institute, Prague (ČHMÚ, 2022). Monthly air temperature and precipitation data from Croatia were provided by the Croatian Meteorological and Hydrological Service (DHMZ, 2022). Monthly air temperature and precipitation data from Italy were provided by the Italian Civil Protection Authority, Region Basilicata (PCRB, 2022). The TSI data were taken from the Solar Influences Data Analysis Center from Royal Observatory of Belgium, Brussels (Dewitte and Nevens, 2016; Dewitte et al., 2022; Royal Observatory of Belgium, 2023). Data on annual and monthly NAO index are calculated from Gibraltar and SW Iceland and were taken from the Climatic Research Unit, University of East Anglia (Jones et al., 1997; CRU-UEA, 2022). Fig. 2 shows the primary precipitation, temperature, TSI, and NAO data, used in this study. This figure also indicates the range between monthly seasonal and of seasonal precipitation to temperature on the plots in CZ, HR and IT.

2.3. Data analysis

Silver fir dendrochronological data were processed in R software (Team R Core, 2022) using the “dplR” package (Bunn, 2008, 2010). The detrending of each tree-ring chronology was conducted by fitting a negative exponential curve with interleaved splines using the "dplR" package instructions (Bunn et al., 2018). This detrending eliminates the age-related trend while retaining low-frequency climate signals (Fritts, 1976; Cook et al., 1990). From detrended tree ring curves, an average tree-ring series was calculated, like a robust mean from individual measured samples, which builds a mean value chronology. An expressed population signal (EPS) was computed for the detrended tree-ring data. The EPS indicates the reliability of a chronology by measuring the proportion of the combined variance within the hypothetical infinite tree population. To ensure data suitability for climate comparison, a significant EPS threshold of EPS > 0.85 was applied (Bunn et al., 2018). We computed various indices to assess the characteristics of the chronology, including the signal-to-noise ratio (SNR) that measures the signal strength, inter-series correlations (R-bar) indicating the relationships between series, and the first-order autocorrelation (Ar1) capturing the temporal dependencies within the series (Fritts, 1976; Wigley et al., 1984). The EPS, SNR, R-bar, and Ar1 indices were computed using the guidelines provided in the "dplR" instructions (Bunn and Korpela, 2018a). These indices are based from known fundamental principles in dendrochronology (Fritts, 1976; Cook et al., 1990; Speer, 2010). A description of the dendrochronological characteristics is provided in Table 3.

Spectral analyses of the data were performed using Statistica 13 software (StatSoft, 2013). The calculation was performed using the “Single Fourier (Spectral) Analysis” function, using the “Periodogram” plot by “Period” output. In addition, correlation coefficients and cross-correlations were calculated using this software, with the threshold for statistically significant correlation results set at standard $p < 0.05$. A wavelet plot was also created using the “signal” and “dplR” software packages for silver fir dendrochronological data for the period 1990 to 2021 (Ligges et al., 2015; Bunn et al., 2018).

Precipitation and temperature analyses are characterized by the

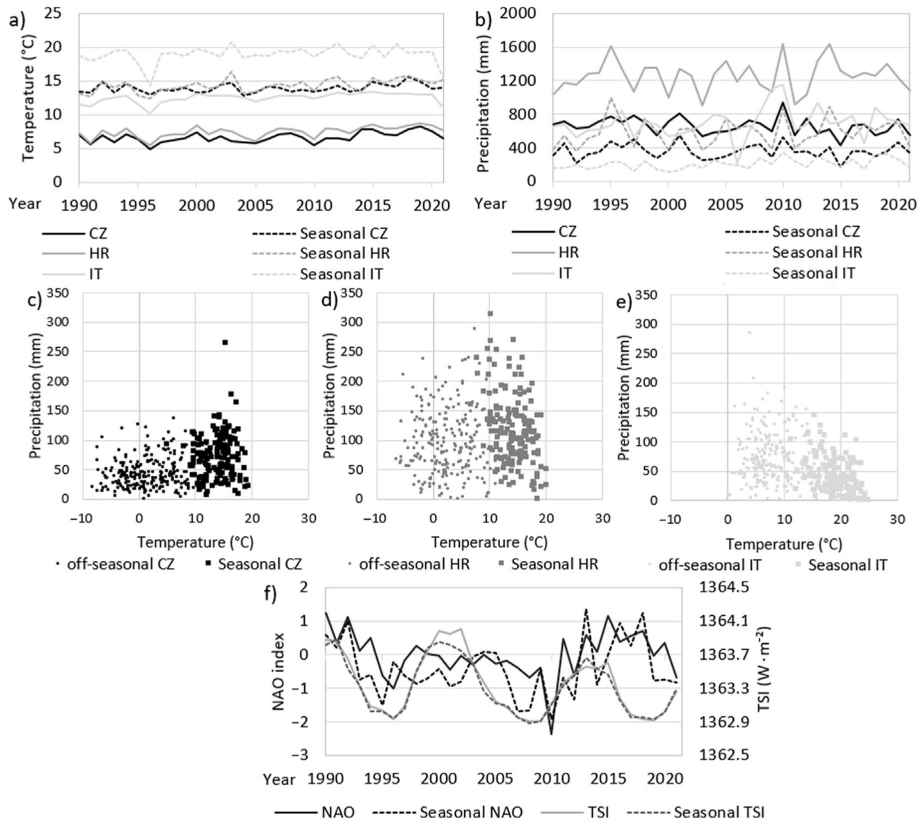

Fig. 2. Institutional or open access data (1990–2021) used in this study: **(a)** Temperature and seasonal temperature of utilized meteorological stations; **(b)** Precipitation and seasonal precipitation from the participating meteorological stations; monthly precipitation to temperature in point graph for seasonal and off-seasonal monthly data for plot **(c)** CZ, **(d)** HR and **(e)** IT; **(f)** NAO index and TSI data.

Table 3
Characteristics of tree-ring chronologies for silver fir for research plots in 1990–2021.

Plot name	No. trees	Mean RW (mm)	SD RW	Mean min–max (mm)	Age min–max	Ar1	R-bar	ESP	SNR
CZ_1	30	2.37	1.09	1.40–4.57	47–76	0.77	0.44	0.96	22.97
CZ_2	32	3.34	1.25	1.94–4.85	42–68	0.67	0.45	0.96	24.98
CZ_3	35	3.28	1.18	2.24–4.96	41–63	0.69	0.45	0.97	29.13
HR_1	33	2.12	1.21	1.42–3.21	51–76	0.70	0.27	0.91	9.52
HR_2	31	2.17	1.26	1.35–2.99	54–75	0.80	0.30	0.91	10.43
HR_3	31	2.21	1.86	1.33–3.18	51–73	0.74	0.30	0.91	10.43
IT_1	33	2.92	1.42	1.85–4.59	38–71	0.71	0.24	0.91	10.61
IT_2	29	3.08	1.76	2.06–4.15	38–66	0.75	0.25	0.90	9.41
IT_3	35	2.33	2.33	1.74–3.40	42–75	0.67	0.41	0.95	18.69

Notes: No. trees—number of trees; Mean RW—mean ring width in mm; SD RW—standard deviation from ring width in mm; Mean min–max—average ring width increment of the smallest and largest of core sample in the plot; Age min–max—age range of youngest and oldest sample tree; Ar1—first order autocorrelation; R-bar—inter-series correlation; EPS—expressed population signal; SNR—signal-to-noise ratio.

nearest climate station for each state (Table 2). The data used for analyses were transformed into yearly sampled (annual interval) data series. The precipitation, temperature and NAO datasets were performed from monthly dataset intervals into the yearly intervals. The monthly data sets were separated into the more detailed factors. The TSI data were acquired as daily records and were converted into monthly values by taking the arithmetic average of all days within a month. We used classical annual data, which represent the arithmetic average the 12 months in the year, and this method was applied to calculate temperature, TSI, and NAO. Precipitation was calculated as the total sum for each of the 12 months in the year. These annual indicators used in our study are described in the results as temperature, precipitation, NAO, and TSI.

The monthly period from May to September was used to calculate the yearly interval seasonal data. Seasonal temperature, seasonal TSI, and seasonal NAO were calculated as the arithmetic mean of the monthly values for those seasonal months. To calculate seasonal precipitation, sums of monthly precipitation totals for the given seasonal periods were used. This seasonal window was intentional to minimize variability in the beginnings and ends of the growing season. Seasonal data evaluated in this time window reflect the actual vegetation period common to all research plots.

The data named as P10–C4 indicates the data interval between the months of October of the previous year to April of the current year while this interval describes cumulative effect in the off-season period. The data named as C6-7 indicates the data interval between the months of June to July in the current year while this data shows the strongest effects during the vegetation period.

The principal component analysis (PCA) was performed in the CANOCO 5 program (Šmilauer and Lepš, 2014) to evaluate the relationships between the radial width index, air temperature, precipitation, total solar irradiance and North Atlantic oscillation for Czechia, Croatia, Italy and all countries together in period 1990–2021. Prior to analysis, the data was standardized, centralized and logarithmized. The results of PCA were presented in a species and environmental variables diagram.

DendroClim 2002 software was used to analyze monthly correlations between the detrended RWI (ring-width index) and temperature, precipitation, NAO index, and TSI. This software was applied to analyze the response and correlation functions during the months from May of the previous relative vegetation season to September of the current relative vegetation season (Biondi and Waikul, 2004). This software operates with RWI (in annual intervals) and compares it with individual monthly data, which are used once per year interval. Through this step, the software creates an average curve for a given month, allowing for a comparable annual interval of RWI with the yearly interval of that month. The advantage of these monthly correlations is that they describe the course of RWI throughout the year, which may be useful in depicting the influence of our studied factors. The benefit of this analysis is that it illustrates how RWI behaves concerning the solar cycle and NAO in monthly intervals, concurrently describing the impact of precipitation and temperature on RWI from the previous growing season to the.

3. Results

3.1. Silver fir tree rings in relation to NAO, TSI and climate

The research plots show different growth of silver fir in the context of latitude over the study period from 1990 to 2021 (Fig. 3). The tree-ring analyses in CZ show a cyclical skewing of the tree-ring series in all research plots, and this skewing is visually replicated in the TSI data (Fig. 3a). However, the similarity to the NAO waveform is smaller in the CZ plots than for the TSI (Fig. 3d). The fluctuations with the TSI during solar cycle are lower in the HR research plots (Fig. 3b), but the waveform of the tree-ring growth reflects the course of the NAO better (Fig. 3e). Research plots in HR are much less cyclic and form shorter fluctuations that vary from year to year. Research plots in IT show the least similarity to the course of the seasonal NAO and TSI (Fig. 3c, f). Regarding fir growth fluctuations, the tree-ring analyses are most balanced in IT and do not show considerable variation among the RWIs.

In terms of NAO indicators, the RWI of research plots in the PCA (Fig. 4a, b, c) indicates that the seasonal NAO index has the highest link with plots in CZ, HR, and IT. High connections of the RWI were also observed with the seasonal NAO for all plots in the overall PCA (Fig. 4d). The influence of NAO C6-7 on the RWI was less pronounced than that of the seasonal NAO. Conversely, the annual NAO had the least impact among the NAO factors.

According to the PCA, all factors of TSI (annual TSI, seasonal TSI, TSI C6-7, and TSI P10–C4) showed the highest link with RWI in research plots in CZ, followed by HR. However, plots in IT exhibited the weakest relationship with TSI indicators and RWI. Consequently, the significance of TSI diminishes in research plots from north to south. In Fig. 4d, representing the overall PCA, TSI emerges as the most influential indicator. Additionally, this figure illustrates that research plots in CZ followed the solar cycle, while plots in HR exhibited an antiphase relationship with the solar cycle according to RWI. Plots in IT did not show a clear link to TSI, and their response to studied factors appeared more random. However, the RWI of plots in IT was more closely related to seasonal temperature and temperature in C6-7, with precipitation in C6-7 and seasonal precipitation emerging as more significant factors compared to TSI in Italian plots.

In almost all countries (Fig. 4a, b, c), seasonal precipitation and precipitation in C6-7 positively associate with RWI, while seasonal temperature and temperature in C6-7 consistently exhibit a negative correspondence. Therefore, temperature during the season consistently emerges as a negative factor for the radial growth of silver fir in all countries.

The RWI tree-ring series are also often influenced by monthly temperature, precipitation, TSI, or NAO, according to the recorded data. Thus, there may be a significant correlation with the RWI data that most influences the tree-ring increment, but often is a combination of several factors (Fig. 5). This graph is intended to demonstrate how the RWI behaves during the pre-growing season and the current growing season against studied factors. The highest observed correlations ($p < 0.05$) between RWI and monthly data were observed for TSI in HR, specifically for HR_1, HR_2, and HR_3. The TSI in HR correlates with RWI in almost all months, with correlations having similar negative results for the current relative and previous vegetation season. Furthermore, many correlations were observed in the CZ research plots. The significant results were recorded in the research plot CZ_1. Research plot CZ_2 recorded the most results during the current vegetation season from June to September, and CZ_3 had a significant result in July and August of the current year. Research plots in IT observed the least values between TSI and RWI. Correlations (positive) were only found for plot IT_2 in September of the current year, and plot IT_3 was correlated (negative) in August of the current year.

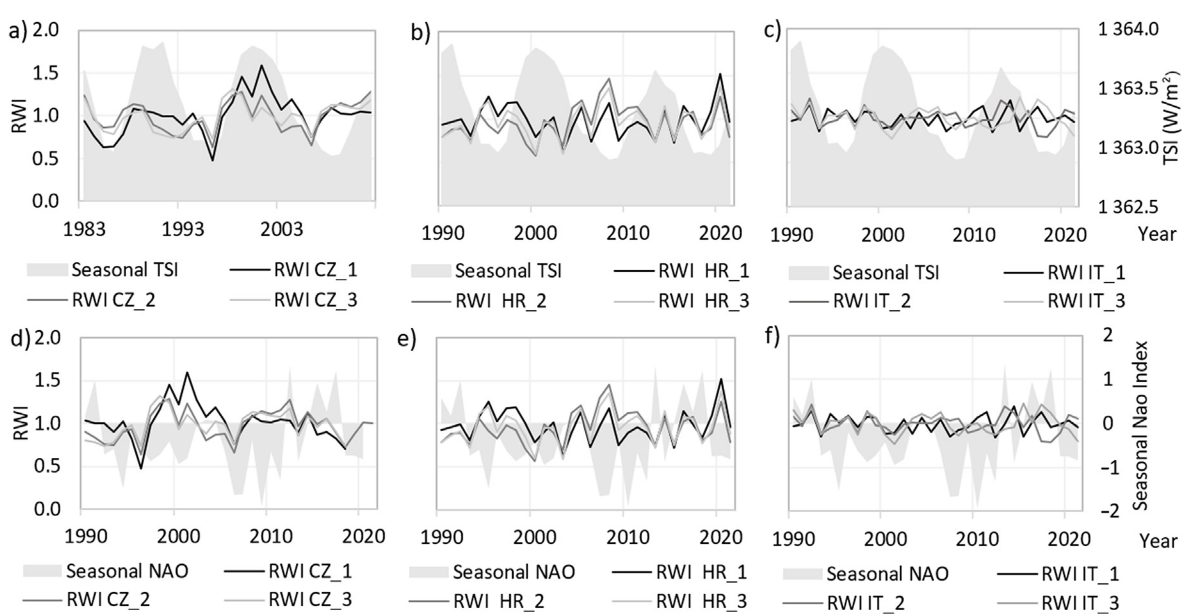

Fig. 3. Ring-width index (RWI) of silver fir on research plots in 1990–2021 compared with TSI number and NAO index: RWI and TSI in research plots in **(a)** Czechia, **(b)** Croatia, **(c)** Italy; RWI and NAO index in **(d)** Czechia, **(e)** Croatia, **(f)** Italy.

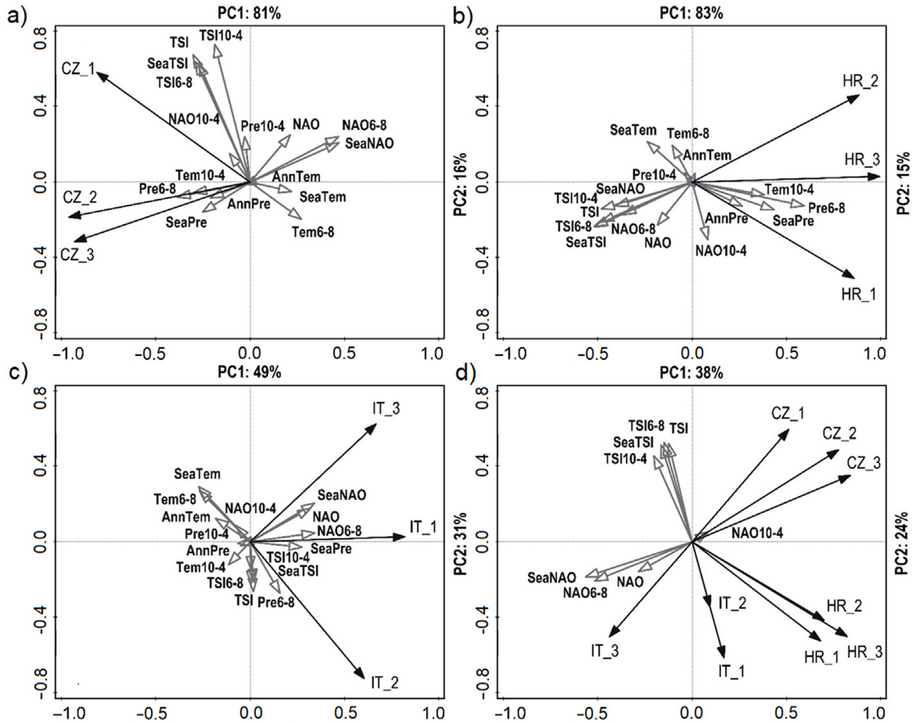

Fig. 4. Ordination diagram showing results of the principal component analysis of relationships between the radial width index (RWI), temperature (TemAnn—annual temperature, TemSea—seasonal temperature, Tem6-8—temperature from June to August of the current year, Tem10-4—temperature from October of the previous year to April of the current year), precipitation (PrecAnn—annual precipitation, PreSea—seasonal precipitation, Pre6-8—precipitation from June to August of the current year, Pre10-4—precipitation from October of the previous year to April of the current year), total solar irradiance (TSI, TSI6-8—total solar irradiance from June to August of the current year, TSI10-4—total solar irradiance from October of the previous year to April of the current year) and North Atlantic oscillation (NAO, NAO6-8—North Atlantic oscillation from June to August of the current year, NAO10-4— North Atlantic oscillation from October of the previous year to April of the current year) for three research plots in Czechia (a), Croatia (b), Italy (c) and all countries (d) in period 1990–2021.

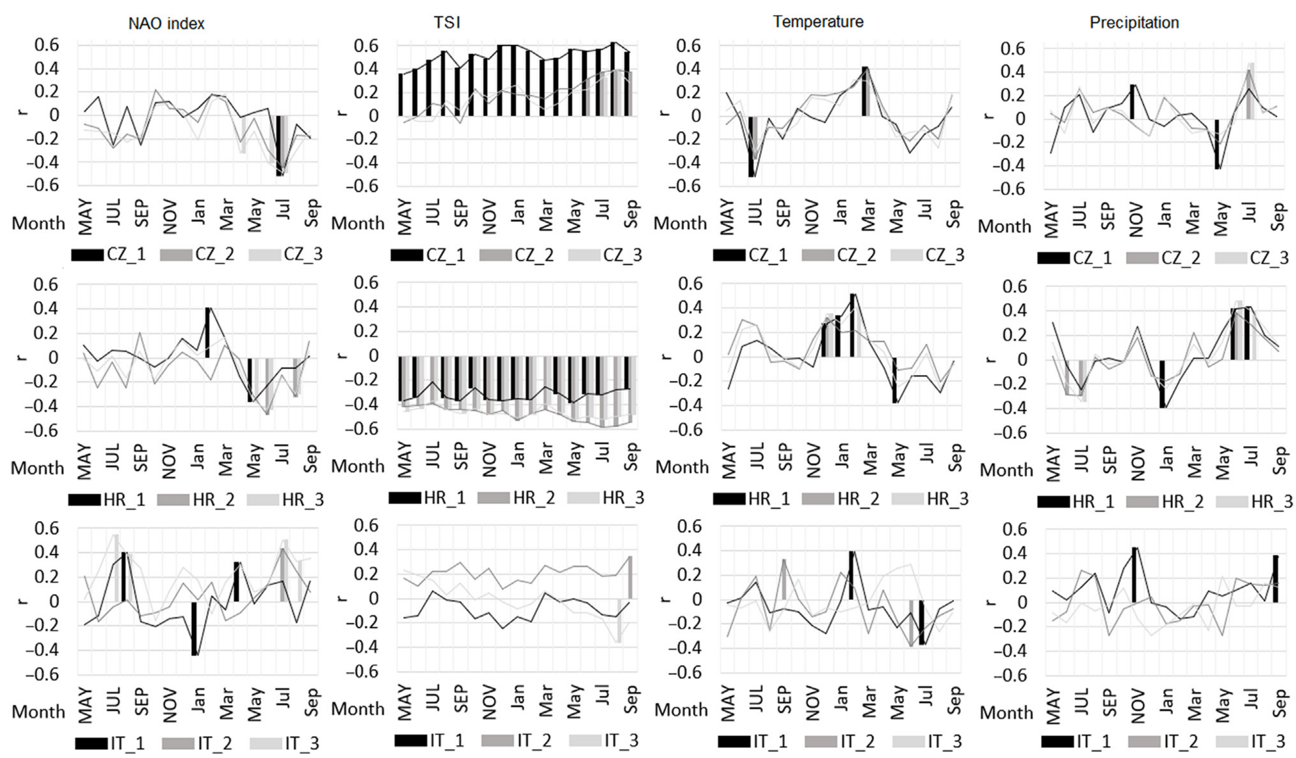

Fig. 5. Correlation coefficients of RWI with monthly NAO index, TSI, temperature, and precipitation from May of the preceding year (all capital letters) to September of the current year (lower case letters) for the period 1990–2021 only correlation coefficients with statistically significant values ($\alpha = 0.05$) are displayed.

The results of RWI and monthly NAO index data show that research plots in CZ and HR are negatively correlated, while they are positively correlated in IT. Most correlations between RWI and NAO are in the months of the vegetation season of the current year for almost all research plots. Most common results between RWI in CZ and NAO were recorded in July when all research plots (CZ_1, CZ_2, and CZ_3) correlated negatively with the NAO index during the current vegetation season. Research plots in HR correlated negatively with NAO from May to June during the current vegetation season. Significant results for HR_1 were found for January and May in the current vegetation season. The HR_2 plot correlates with NAO in June and August. The HR_3 plot correlates in May, June, and August. The study areas in IT correlate positively with NAO, and significant results can be found in the previous vegetation season. However, these IT plots have fewer common significant months. July and August of the previous and current vegetation seasons for IT_1 and IT_3 are worth mentioning.

Monthly precipitation is most similar to the NAO index and RWI correlations, where significant values in June, July, and August show opposite correlations to the NAO index. Concerning the NAO to RWI correlations, these precipitation values may vary from plot to plot. In general, precipitation most significantly affects fir growth in July. The correlations of monthly temperatures to RWI are observed primarily at the beginning of the vegetation season and even outside of it, where positive correlations are observed from January to March. For temperatures, positive correlations are recorded outside the vegetation season for all three states surveyed. In the research plots HR_1 (May), IT_1 (July), and IT_2 (June), negative correlations are recorded with average monthly temperatures during the vegetation season. Monthly temperatures are predominantly negatively correlated with RWI across all plots during the growing season, whereas monthly precipitation totals mainly exhibit positive correlations with RWI during the growing season. Some plots are statistically significant with precipitation and temperature, some are not, but the overall trend is evident from the results.

3.2. Cyclical tree-ring growth of silver fir from north to south

The spectral analysis in Fig. 6 reveals that the research plots in the CZ and their RWI undergo the longest cycles, reaching values up to 0.30 on the Periodogram Values axis at period nine or further. These 9+ year cycles are the longest for the CZ plots (the northernmost plots), with the short-term 3 to 5-year cycles being much smaller. Research plots in HR experience more noticeable short-term cycles of around three to four periods but reach the highest values on the Periodogram Values axis (up to 0.45). Other cycles in HR are shorter and less intense when compared to plots in CZ. However, the research plots in HR also experience 9 to 16-year cycles that are smaller in terms of Periodogram values (up to 0.21). The research plots in IT are the lowest in cyclicity and show different periods in the RWI growth compared to the plots in HR and CZ. The research plots in IT show 2 to 8-year cycles in RWI and are up to 0.11 regarding the Periodogram Values axis, which is almost three times smaller compared to CZ and HR. Thus, in the IT plots, the increase in RWI is non-cyclical compared to HR and especially CZ.

The wavelet power spectrum analysis in Fig. 7 shows that the research plots have different cycles of RWI, but each state is characterized by its basic periodic features. The research plots in CZ observed from 9 to 14-year cycles. These observed cycles can be found in almost all CZ research plots. The least observed is CZ_2 from 1990 to 2015, followed by CZ_1 (significant cycle from 1997 to 2008), and the least cyclical variability is CZ_3 (significant cycle from 1995 to 2005). The RWI research plots in HR experienced minor cyclical fluctuations that are below the level of statistical significance and only observed 3.1-year periods for plot HR_3. Research plots in HR are also characterized by 2 to 4-year cycles that are less apparent than those in CZ. Research plots in IT show the most divergent spectral analysis results. However, there are also

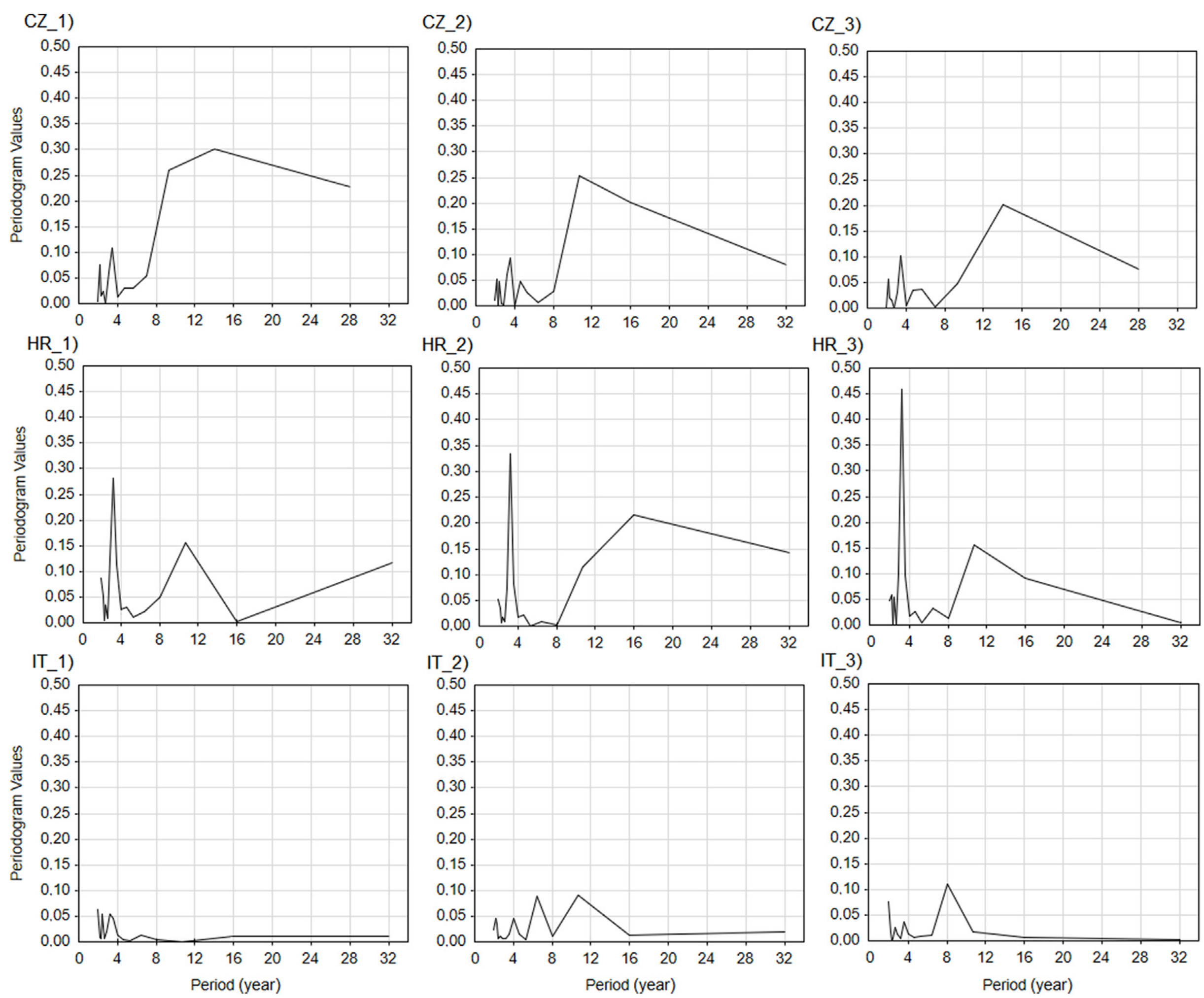

Fig. 6. Single spectral analysis of silver fir RWI research plots in 1990–2021.

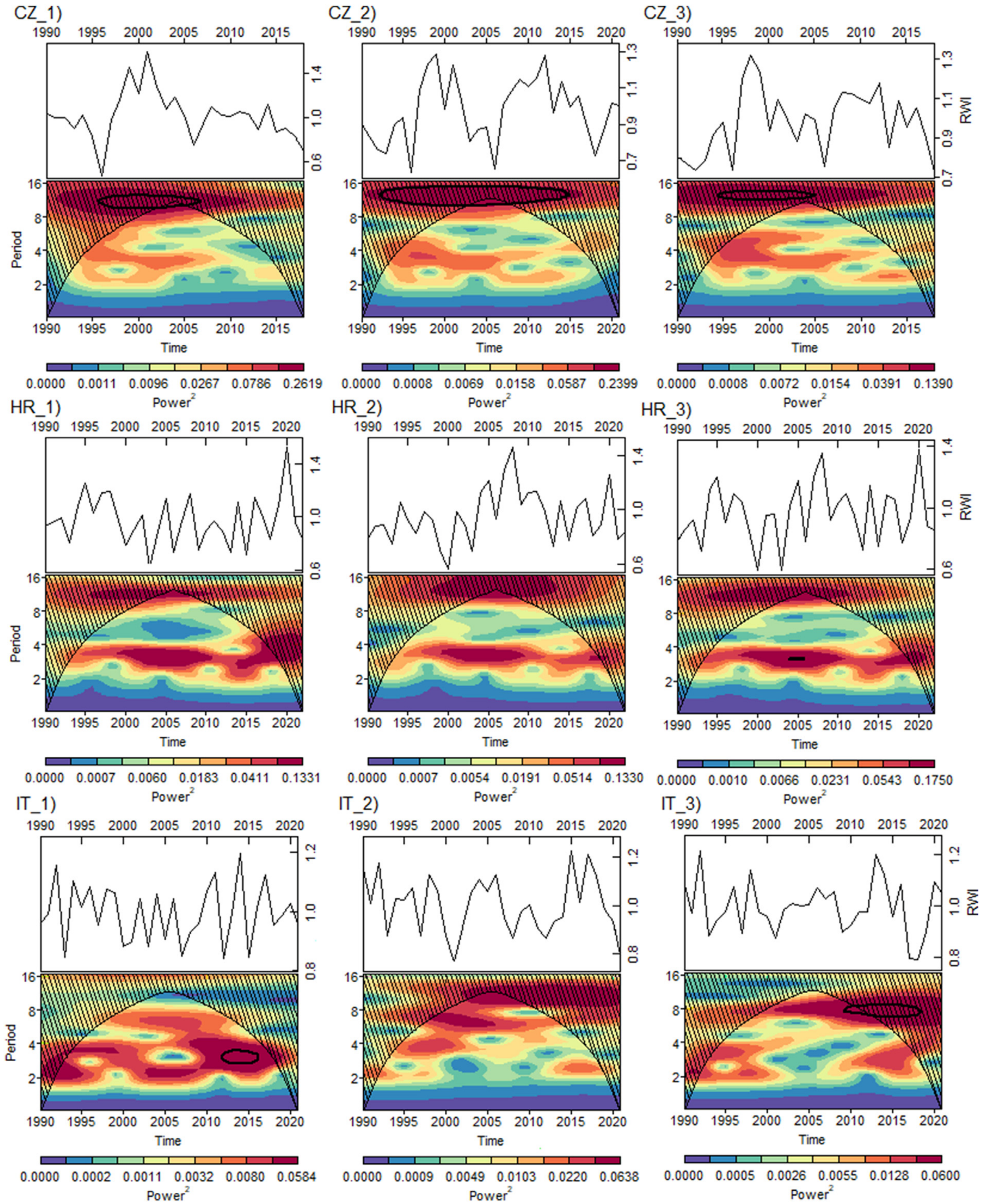

Fig. 7. Wavelet power spectrum for silver fir RWI research plots from 1990 to 2021. The thick black line represents the 95% significance level against the noise level. Power^2 describes a relative unit of variance comparable to time series.

observed 3 to 4-year cycles for IT_1 circa 2015. For plot IT_3, an observation of cycle is found from 2010 to 2018 in a 9 to 7-year period. In this context, it should be noted that the wavelet analysis shows comparative results that are not common to all plots and only significant results are shown here.

4. Discussion

4.1. Growth conditions for silver fir from Central Europe to the mediterranean

The results of this study clearly show that silver fir tree-ring increments react in all research plots with both TSI and NAO index, more than temperature and precipitation. The highest reaction with the TSI has even been recorded in the northernmost research plots in CZ and decreased southward across HR and IT (Fig. 4d). In Czechia and Croatia, the precipitation is concentrated mainly during the vegetation season, while in contrast, in the Italian experimental plots (Figs. 1 and 2), the highest precipitation comes during the winter season. Monthly precipitation (according to Fig. 1) varies during the growing season from May to September, ranging from 65 to 88 mm for CZ, 109–115 mm for HR, and 26–52 mm for IT (which is the opposite of the patterns observed in CZ and HR) on average during the month. It can be suggested that when precipitation is more influenced by NAO than temperature (Kjellström et al., 2013; Laurenz et al., 2019), this phenomenon most likely influences the occurrence of dry periods that negatively affects tree-ring growth. In addition, there is also a strong link between drought variability in Europe and NAO (Vicente-Serrano et al., 2011, 2016). Cold extremes may play an additional role in the variation of the tree-ring analyses in Central Europe, thus being bigger than warm extremes in terms of deviations from the monthly average (Diao et al., 2015), which is supported by Figs. 1 and 2, where the CZ climate station shows the lowest temperatures and is also the northernmost in the lowest altitude.

The influence of the solar cycle through TSI and the NAO index can be observed from the results of this study. These are the different factors that determine the variability of fir growth, primarily in Central Europe in the research plots from CZ and HR. In IT, the research plots also show stable development and a steady decrease in growth. The studied tree-ring series are also influenced by NAO, which are highly linked with research plots in each of the studied countries. In the Mediterranean, fir decline has been observed in recent years due to increased environmental aridity (Gazol et al., 2019), but results from our mountain sites in IT show that fir has stable non-cyclical increments compared to plots in HR and CZ. Since 1980, there has been a stronger response of tree-ring growth to the NAO, which mainly influences local seasonal climate, especially winter temperatures, which has been observed for spruce in Canada and Sweden, for example (Ols et al., 2018). The effect of NAO has shortened in recent years in Central Europe and reduced winter periods (Hernández-Almeida et al., 2015). Understandably, winter frosts are responsible for the reduced growth of silver fir in mountain areas (Mauri et al., 2016; Jarzyna, 2021).

In the Mediterranean, tree-ring series are typically limited by high summer temperature, which has a delayed effect on tree growth. Fir is a tree species that is poorly adapted to warm and summer drought conditions (Nussbaumer et al., 2020; Walder et al., 2021), as confirmed in Figs. 4 and 5, where research plots in IT and HR show a high opposite trend with seasonal temperatures and temperature in mainly current June and July (also can be seen in season) while precipitation has a positive effect. With respect to monthly temperature distribution, the areas in IT are more negatively affected, where negative correlations are observed in May and June. The dry conditions prevailing during the positive phases of the winter NAO have had a significant negative effect on the plots located in the western and central Mediterranean, where the influence of NAO has generally decreased over the last six decades (Chen et al., 2015). Overall, a significant limiting factor for fir growth has been the lack of summer precipitation, particularly in July (which confirmed also PCA for precipitation in current June to July). Similarly, other studies have documented that June and July are the most important months in terms of the influence of climatic factors on fir radial growth and cell production of wood formation (Maxime and Hendrik, 2011; Cuny et al., 2013).

Precipitation during the growing season positively influences the radial growth of fir trees, while temperatures exhibit a negative impact on growth during season and individual months across all research plots along the meridian. This indicates the dependence of fir trees on precipitation management. Conversely, higher temperatures during the season often result in increased evaporation, intensifying drought conditions for fir growth during the growing period. The positive effect of precipitation and the negative impact of temperatures during the summer season is a well-established phenomenon, widely documented, for instance, in France (Lebourgeois et al., 2010). Similar outcomes regarding the influence of temperature and precipitation during the growing season on silver fir have been observed in Spain and Italy (Gazol et al., 2015). It can be concluded that this pattern of precipitation and temperature is a consistent phenomenon across Europe.

4.2. The solar cycle like a most visible cycle in silver fir tree rings across latitude

Since 1990, the solar cycle has been present in silver fir tree-rings across the results of PCA, but the 11-year cycle is also present in RWI spectral wavelet analyses across the experimental plots. According to the spectral analysis, research plots in CZ peak in cycles from 9 to 14 years, while plots in HR peak in 9 to 16-year cycles, and in IT, the research plots peak in 8 to 9-year cycles in two out of three cases. However, depending on the annual duration, the solar cycle can be from 8 to 14 years long (Hathaway, 2015), which is very close to the results of the silver fir RWI spectral analysis across the meridian. The observation of the solar cycle can be explained by several factors acting in different forms on tree growth across the meridian, where a common factor for all states could be the influence of the TSI, for example. TSI shows the variability of radiation reaching the surface of the planet, and 0.1% of it is merely the 11-year cycle, which is higher during the solar maximum (Kopp, 2021). Not only TSI but also the entire light spectrum shows a strong correlation with the wavelength of solar irradiance during the solar cycle TSI (Tsiropoula, 2003; Woods et al., 2022). The solar cycle also accompanies the cosmic radiation cycle, which influences the formation of cloud cover during minimum solar activity, resulting in an increase in the albedo effect, and thus, possible climate cooling. But this effect is not large enough to change the current climate situation (Ormes, 2018). Linked to the solar cycle is the circulation of water flow on the planet (Al-Tameemi and Chukin, 2016), and this is directly observed before NAO in the precipitation and temperature cycle over the entire European continent (Laurenz et al., 2019; Lüdecke et al., 2020).

The Top-down (direct solar irradiance variability) mechanism in solar forcing, in our view, exerts a relatively smaller effect on our studied tree-ring series. It is noteworthy that the inverse influence between the plots in CZ and HR concerning TSI aligns with the theory of the Bottom-up mechanism of solar influence on European ecosystems (Gray et al., 2010; Muraki et al., 2011). In this context, the NAO circulation emerges as a pivotal cyclic mechanism governing surface weather patterns on our planet (Smith et al., 2019, 2020). This suggests that the NAO may play a more significant role in shaping the climate and, subsequently, the growth of tree-ring series in our study. Thanks to the positive influence of TSI in CZ (positive phase) and the negative impact of the solar cycle in HR (antiphase), we can infer that these types of oscillations may create different conditions for forest growth within the framework of the solar cycle. However, this effect may also appear counterintuitive depending on the location of occurrence.

Due to the cyclic changes in wind pattern oscillations within the NAO, we lean towards a combination of solar cycle which influences are manifested through precipitation and temperatures on tree-ring series. Therefore, the white fir reacts similarly to both seasonal precipitation and temperatures across the meridian, as it thrives on having sufficient moisture during the season. However, higher temperatures alter humidity conditions, creating drier periods, which in turn affect fir growth that can by cyclically different across the meridian but causes of high or low ring increment are still preserved.

Regarding the solar cycle, the most frequent studies on the European continent have been performed with the annual growth of beech, which shows a relationship with the sunspot number in Czechia, Italy (Šimůnek et al., 2020a, 2021b), and Bulgaria (Komitov, 2021). The solar cycle has also been described in studies on Scots pine (*Pinus sylvestris* L.) in Russia and Slovakia (Shumilov et al., 2011; Dorotovič et al., 2014; Matveev et al., 2017; Kasatkina et al., 2019). Nevertheless, it is imperative to note that the influence of the solar cycle on tree rings has not been extensively explored on a larger geographical scale studies in Europe.

The impact of latitude on the length of the sunlight day and its effects on tree ring growth is an important factor to consider in understanding growth variability and cyclicity. Research findings in northern China, situated at higher latitudes, reveal the effect of the sunshine daytime on tree-ring growth. The research showed an important link between the temperature and sunlight duration hours that can lead to vapor pressure deficit which affects tree-ring growth (Li et al., 2022). The dependence of tree ring growth variability on the latitude length is not connected to the impact of drought on tree-level resilience (Bose et al., 2020). Furthermore, investigated trees across a North American latitudinal gradient, establishing a positive correlation between tree ring width and day length while highlighting the critical role of daylight duration in shaping tree ring formation (Johnson et al., 2016).

Our findings indicate that the largest cycles are recorded in growth patterns in the northernmost research plots in the CZ, followed by plots in HR, where fluctuations are lower, but the trend of tree ring variability is more of a decadal nature. In contrast, growth variations on research plots in Italy (IT) are minimal. The length of the daylight day remains a relatively constant factor for each year. We must also note that with increasing elevation, meaning as forests ascend to higher altitudes, the impact of solar radiation on tree growth, coupled with temperature, becomes more significant (Černý et al., 2020). However, the more we go to south, the less TSI is shown to be an important factor for tree growth, where in IT (the highest research altitude) there is a more subtle connection with the growth of RWI than in CZ, where the altitude of the research plots is the lowest.

This effect of the largest growth cycles being more pronounced from north to south could also be accentuated by the contrast between continental and Mediterranean climates. Trees in the Mediterranean climate, characterized by hot dry summers and mild rainy winters, exhibit specific patterns in their tree-ring growth. Increased growth often occurs during periods with sufficient precipitation, typically limited to the winter months. Conversely, in a continental climate with more pronounced temperature extremes between summer and winter, tree-ring series are influenced differently. Studies indicate that trees in continental regions may tend to show greater variability in their growth. (St. George, 2014). However, mountain Mediterranean climates may be more sensitive to drought, but mountain conditions in turn reduce this drought effect (Bhuyan et al., 2017). While the plots in Italy show less cyclic growth, they are, in fact, situated at the highest altitudes.

Climate change in recent years has been primarily caused by rising global temperatures, which increase tree-ring increment in mountainous areas (Ponocná et al., 2018; Šimůnek et al., 2019). However, mid- and low-altitude forest environments are more susceptible to fluctuations in climatic conditions, and thus, for example, cyclical recurrence of bark beetle calamities or droughts may occur (Heinimann, 2010; Maxime and Hendrik, 2011; Milad et al., 2011). In this study, the solar cycle is confirmed for silver fir tree rings in CZ and HR but can also be found in the cycle of salvage harvests in CZ, which multiply the devastation caused by severe droughts due to rising temperatures and uneven distribution of precipitation over the vegetation season (Šimůnek et al., 2020b, 2021a). Moreover, due to the low cyclicity of IT research plots, it can be theorized that cyclic forestry problems in southern Italy are less substantial than those in Central Europe.

4.3. *Silver fir in the recent years of the climate change and its time series limits*

This study describes the tree-ring growth of fir since 1990, which covers the least-biased period of fir tree-ring series in the research plots. This period in the tree-ring series of the research plots has not experienced significant economic interventions, and the plots in CZ are also no longer affected by any distinctive air pollution, which significantly influenced or even degraded fir stands in the past (Łuszczyńska et al., 2018; Mikulenka et al., 2020). This degradation of silver fir by air pollution (particularly SO_2) lasted until the 1980s (Elling et al., 2009), so it can be assumed that stands from the 1990s onwards were no longer significantly affected.

Firs are not only sensitive to air pollution but also to climate change, i.e., long periods of drought or temperature fluctuations (Bert, 1993; Gazol et al., 2015). The consequences of rising temperatures have been visible in our research, especially since 2000, when temperature trends in Europe started to rise significantly (Naumann et al., 2021). This period has therefore caused divergences in tree-ring increment to other factors tracked through the course of climate change (Conte et al., 2018; Ponocná et al., 2018; Ahmed et al., 2020; Li et al., 2023). Since 1990, tree-ring divergence in response to climate events has become increasingly apparent (D'Arrigo et al., 2008; Zhang et al., 2018; Li et al., 2023). However, the response of tree-ring growth to climate fluctuations can vary substantially. Previous dendrochronological studies confirmed the considerable adaptation of silver fir to warmer temperatures (Štefančík et al., 2018; Walder et al., 2021) and demonstrated more drought tolerance than expected (Vitali et al., 2017).

However, climate change may reduce the abundance of silver fir and considerably affect its range (Dobrowolska et al., 2017), but a shift in the distribution of fir towards higher altitudes and northward is predicted (Büntgen et al., 2014; Klopčič et al., 2017). The effect of elevation on the occurrence of silver fir in our research ranges from 660 to 1,324 m, with the lowest plots in CZ and the highest in IT. This indicates that silver fir thrives in the south, especially in mountainous regions, where higher elevations compensate for the increase in temperatures further south along the meridian. An interesting example is that temperatures in CZ and HR are very similar, despite a 395 m difference in elevation between meteorological stations. Even in the Italian research plots with the highest altitude, variability of fir growth and negative effect of high temperatures are evident. On the other hand, the genetic diversity and provenance of fir trees also play a crucial role, where some populations are very tolerant to drought and may also reach high production potential (Teodosiu et al., 2019; Mihai et al., 2021).

By reducing the growth of RWI since 1990, it was possible to better describe the factors influencing the growth of silver fir along the meridian during climate change, while the data was not affected by the pollution load.

5. Conclusion

The results of this dendrochronological study show that silver firs' increment has been different across the research plots from Central to Southern Europe around the 16th meridian in the period since 1990 when ongoing climate change and extreme temperature fluctuations became more pronounced. Of the factors investigated, the greatest influence was shown to be a seasonal NAO index and TSI. An important result is also the negative impact of seasonal temperatures and temperatures during the months of June and July, as well as the positive influence of seasonal precipitation totals during the months of June and July on all studied plots. Monthly temperatures correlate with tree-ring increment RWI at the beginning of the vegetation season, while precipitation during the summer, and the weather in July and specially in current June to July play the leading role regarding tree-ring increment. The most prominent interaction between the TSI and RWI is observed in CZ and decreases toward the south. The TSI may have varying effects, with a positive impact in the CZ and simultaneously a negative influence in HR, while it tends to be more neutral in IT. On the other hand, seasonal NAO tends to negatively impact the silver fir's RWI in HR and CZ, while in IT, it has a slightly positive effect. Fir shows a highly observed cyclical increment in the northern range of its distribution in CZ as the cyclical pattern and variation along the meridian to the south disappear, demonstrating the association of cycles with the influence of seasonal NAO and TSI. Thus, our research suggests that silver fir growth is systematically influenced by the parameters examined across the north-south range of its distribution. The findings of this study can be applied as a basis for long-term planning in forest management to determine recurring cyclic events. However, it is essential to focus on suitable provenances, silvicultural practices, and other factors affecting the growth and distribution of this historically abundant tree species in the context of changing environmental conditions.

Funding

This study was supported by the Czech University of Life Sciences Prague, Faculty of Forestry and Wood Sciences (No. IGA A_21_26) and the Ministry of Agriculture of the Czech Republic (No. QK1910292 and QK21020371).

Availability of data and materials

The monthly air temperature and precipitation data for Czechia were from Czech Hydrometeorological Institute, Prague. (ČHMÚ, 2022). Monthly air temperature and precipitation data from Croatia were from Croatian Meteorological and Hydrological Service, Zagreb (DHMZ, 2022). Monthly air temperature and precipitation data from Italy were from Italian Civil Protection Authority, Region Basilicata (PCRB, 2022). The TSI data were from Solar Influences Data Analysis Center from Royal Observatory of Belgium, Brussels (Royal Observatory of Belgium, 2023). The NAO index data are from the Climatic Research Unit, University of East Anglia (CRU-UEA, 2022).

Credit authorship contribution statement

Václav Šimůnek: Conceptualization, Data curation, Formal analysis, Investigation, Methodology, Resources, Software, Supervision, Validation, Visualization, Writing – original draft, Writing – review & editing. **Anna Prokůpková:** Investigation, Project administration, Resources, Writing – original draft, Writing – review & editing. **Zdeněk Vacek:** Conceptualization, Data curation, Formal analysis, Funding acquisition, Investigation, Methodology, Resources, Software, Supervision, Visualization, Writing – original draft, Writing – review & editing. **Stanislav Vacek:** Conceptualization, Formal analysis, Methodology, Writing – original draft, Writing – review & editing. **Jan Cukor:** Conceptualization, Investigation, Writing – original draft. **Jiří Remeš:** Conceptualization, Investigation, Project administration, Resources, Writing – original draft. **Vojtěch Hájek:** Data curation, Investigation, Methodology, Software. **Giuseppe D'Andrea:** Data curation, Investigation. **Martin Šálek:** Data curation, Writing – original draft. **Paola Nola:** Investigation, Writing – original draft. **Osvaldo Pericolo:** Writing – original draft, Writing – review & editing. **Šárka Holzbachová:** Data curation, Formal analysis. **Francesco Ripullone:** Conceptualization, Investigation, Writing – original draft.

Declaration of competing interest

The authors declare that they have no known competing financial interests or personal relationships that could have appeared to influence the work reported in this paper.

Acknowledgements

We would like to thank Richard Lee Manore, a native speaker, and Jitka Šišáková, an expert in the field, for checking English. We are also grateful to the Czech Hydrometeorological Institute of the Czech Republic, to Croatian Meteorological and Hydrological Service, and to Italian Civil Protection Authority, Region Basilicata for providing the data for monthly precipitation and temperature; to the Royal Observatory of Belgium, Solar Influences Data Analysis Center for providing the TSI data, to the Climatic Research Unit, University of East Anglia for providing data of monthly NAO index.

References

Ahmed, F., Adnan, S., Latif, M., 2020. Impact of jet stream and associated mechanisms on winter precipitation in Pakistan. Meteorol. Atmos. Phys. 132, 225–238. https://doi.org/10.1007/s00703-019-00683-8.

Akhmetzyanov, L., Sánchez-Salguero, R., García-González, I., Domínguez-Delmás, M., Sass-Klaassen, U., 2023. Blue is the fashion in Mediterranean pines: new drought signals from tree-ring density in southern Europe. Sci. Total Environ. 856, 1–15. https://doi.org/10.1016/j.scitotenv.2022.159291.

Al-Tameemi, M.A., Chukin, V.V., 2016. Global water cycle and solar activity variations. J. Atmos. Sol. Terr. Phys. 142, 55–59. https://doi.org/10.1016/j.jastp.2016.02.023.

Anić, I., Vukelić, J., Mikać, S., Bakšić, D., Ugarković, D., 2009. Utjecaj globalnih klimatskih promjena na ekološku nišu obične jele (*Abies alba* Mill.) u hrvatskoj. Sumar List 133, 135–144.

Bert, G.D., 1993. Impact of ecological factors, climatic stresses, and pollution on growth and health of silver fir (*Abies alba* Mill.) in the Jura Mountains: an ecological and dendrochronological study. Acta Oecol. 14, 229–246.

Bhuyan, U., Zang, C., Menzel, A., 2017. Different responses of multispecies tree ring growth to various drought indices across Europe. Dendrochronologia 44, 1–8. https://doi.org/10.1016/j.dendro.2017.02.002.

Bice, D., Montanari, A., Vučetić, V., Vučetić, M., 2012. The influence of regional and global climatic oscillations on Croatian climate. Int. J. Climatol. 32, 1537–1557. https://doi.org/10.1002/joc.2372.

Biondi, F., Waikul, K., 2004. DENDROCLIM2002: a C++ program for statistical calibration of climate signals in tree-ring chronologies. Comput. Geosci. 30, 303–311. https://doi.org/10.1016/j.cageo.2003.11.004.

Bose, A.K., Gessler, A., Bolte, A., Bottero, A., Buras, A., Cailleret, M., Camarero, J.J., Haeni, M., Heres, A.M., Hevia, A., Lévesque, M., Linares, J.C., Martinez-Vilalta, J., Matías, L., Menzel, A., Sánchez-Salguero, R., Saurer, M., Vennetier, M., Ziche, D., Rigling, A., 2020. Growth and resilience responses of Scots pine to extreme droughts across Europe depend on predrought growth conditions. Glob. Chang. Biol. 26, 4521–4537. https://doi.org/10.1111/gcb.15153.

Bosela, M., Kulla, L., Roessiger, J., Šebeň, V., Dobor, L., Büntgen, U., Lukac, M., 2019. Long-term effects of environmental change and species diversity on tree radial growth in a mixed European forest. For. Ecol. Manag. 446, 293–303. https://doi.org/10.1016/j.foreco.2019.05.033.

Bunn, A.G., 2008. A dendrochronology program library in R (dplR). Dendrochronologia 26, 115–124. https://doi.org/10.1016/j.dendro.2008.01.002.

Bunn, A.G., 2010. Statistical and visual crossdating in R using the dplR library. Dendrochronologia 28, 251–258. https://doi.org/10.1016/j.dendro.2009.12.001.

Bunn, A., Korpela, M., 2018a. An Introduction to dplR. http://cran.nexr.com/web/packages/dplR/vignettes/intro-dplR.pdf. (Accessed 1 October 2023).

Bunn, A., Mikko, K., Biondi, F., Campelo, F., Mérian, P., Qeadan, F., Zang, C., Pucha-Cofrep, D., Wernicke, J., 2018. Dendrochronology Program Library in R. R Package. Dendrochronologia, version 1.6.8.

Büntgen, U., Frank, D., Neuenschwander, T., Esper, J., 2012. Fading temperature sensitivity of Alpine tree growth at its Mediterranean margin and associated effects on large-scale climate reconstructions. Clim. Chang. 114, 651–666. https://doi.org/10.1007/s10584-012-0450-4.

Büntgen, U., Tegel, W., Kaplan, J.O., Schaub, M., Hagedorn, F., Bürgi, M., Brázdil, R., Helle, G., Carrer, M., Heussner, K.U., Hofmann, J., Kontic, R., Kyncl, T., Kyncl, J., Camarero, J.J., Tinner, W., Esper, J., Liebhold, A., 2014. Placing unprecedented recent fir growth in a European-wide and Holocene-long context. Front. Ecol. Environ. 12, 100–106. https://doi.org/10.1890/130089.

Caudullo, G., Tinner, W., de Rigo, D., 2016. *Picea abies* in Europe: distribution, habitat, usage and threats. In: San-Miguel-Ayanz, J., de Rigo, D., Caudullo, G., Houston Durrant, T., Mauri, A. (Eds.), European Atlas of Forest Tree Species. Publication Office of the European Union, Luxembourg, pp. 114–116.

Černý, J., Pokorný, R., Vejpustková, M., Šrámek, V., Bednář, P., 2020. Air temperature is the main driving factor of radiation use efficiency and carbon storage of mature Norway spruce stands under global climate change. Int. J. Biometeorol. 64, 1599–1611. https://doi.org/10.1007/s00484-020-01941-w.

Chen, K., Dorado-Liñán, I., Akhmetzyanov, L., Gea-Izquierdo, G., Zlatanov, T., Menzel, A., 2015. Influence of climate drivers and the North Atlantic oscillation on beech growth at marginal sites across the mediterranean. Clim. Res. 66, 229–242. https://doi.org/10.3354/cr01345.

ČHMÚ, 2022. Czech Hydrometeorological Institute. http://portal.chmi.cz/historicka-data/pocasi/uzemni-srazky. (Accessed 1 October 2022).

Conte, E., Lombardi, F., Battipaglia, G., Palombo, C., Altieri, S., La Porta, N., Marchetti, M., Tognetti, R., 2018. Growth dynamics, climate sensitivity and water use efficiency in pure vs. mixed pine and beech stands in Trentino (Italy). For. Ecol. Manag. 409, 707–718. https://doi.org/10.1016/j.foreco.2017.12.011.

Cook, E.R., Shiyatov, S.G., Mazepa, V.S., 1990. Estimation of the mean chronology. In: Cook, E.R., Kairiukstis, L.A. (Eds.), Methods of Dendrochronology Applications. Columbia University, New York.

CRU-UEA, 2022. North Atlantic Oscillation (NAO) Data. Climatic Research Unit, University of East Anglia. https://crudata.uea.ac.uk/cru/data/nao/index.htm. (Accessed 10 November 2022).

Cuny, H.E., Rathgeber, C.B.K., Kiessé, T.S., Hartmann, F.P., Barbeito, I., Fournier, M., 2013. Generalized additive models reveal the intrinsic complexity of wood formation dynamics. J. Exp. Bot. 64, 1983–1994. https://doi.org/10.1093/jxb/ert057.

Dewitte, S., Nevens, S., 2016. The total solar irradiance climate data record. Astrophys. J. 830, 25. https://doi.org/10.3847/0004-637x/830/1/25.

Dewitte, S., Cornelis, J., Meftah, M., 2022. Centennial total solar irradiance variation. Rem. Sens. 14, 1–12. https://doi.org/10.3390/rs14051072.

DHMZ, 2022. Croatian Meteorological and Hydrological Service. https://meteo.hr/index_en.php. (Accessed 10 November 2022).

Di Filippo, A., Biondi, F., Čufar, K., De Luis, M., Grabner, M., Maugeri, M., Saba, E.P., Schirone, B., Piovesan, G., 2007. Bioclimatology of beech (*Fagus sylvatica* L.) in the Eastern Alps: spatial and altitudinal climatic signals identified through a tree-ring network. J. Biogeogr. 34, 1873–1892. https://doi.org/10.1111/j.1365-2699.2007.01747.x.

Diao, Y., Xie, S.P., Luo, D., 2015. Asymmetry of winter European surface air temperature extremes and the North Atlantic Oscillation. J. Clim. 28, 517–530. https://doi.org/10.1175/JCLI-D-13-00642.1.

Dobrowolska, D., Bončina, A., Klumpp, R., 2017. Ecology and silviculture of silver fir (*Abies alba* Mill.): a review. J. For. Res. 22, 326–335. https://doi.org/10.1080/13416979.2017.1386021.

Dorotovič, I., Louzada, J.L., Rodrigues, J.C., Karlovský, V., 2014. Impact of solar activity on the growth of pine trees (*Pinus cembra*: 1610–1970; *Pinus pinaster*: 1910–1989). Eur. J. For. Res. 133, 639–648. https://doi.org/10.1007/s10342-014-0792-8.

D'Arrigo, R., Wilson, R., Liepert, B., Cherubini, P., 2008. On the "Divergence Problem" in Northern Forests: a review of the tree-ring evidence and possible causes. Glob. Planet. Chang. 60, 289–305. https://doi.org/10.1016/j.gloplacha.2007.03.004.

Elling, W., Dittmar, C., Pfaffelmoser, K., Rötzer, T., 2009. Dendroecological assessment of the complex causes of decline and recovery of the growth of silver fir (*Abies alba* Mill.) in Southern Germany. For. Ecol. Manag. 257, 1175–1187. https://doi.org/10.1016/j.foreco.2008.10.014.

Esper, J., Cook, E.R., Schweingruber, F.H., 2002. Low-frequency signals in long tree-ring chronologies for reconstructing past temperature variability. Science 295, 2250–2253. https://doi.org/10.1126/science.1066208.

Fritts, H.C., 1976. Tree Rings and Climate. Academic Press Inc., Tucson, Arizona, U.S.A.

Gazol, A., Camarero, J.J., Gutiérrez, E., Popa, I., Andreu-Hayles, L., Motta, R., Nola, P., Ribas, M., Sangüesa-Barreda, G., Urbinati, C., Carrer, M., 2015. Distinct effects of climate warming on populations of silver fir (*Abies alba*) across Europe. J. Biogeogr. 42, 1150–1162. https://doi.org/10.1111/jbi.12512.

Gazol, A., Camarero, J.J., Colangelo, M., de Luis, M., del Castillo, E.M., Serra-Maluquer, X., 2019. Summer drought and spring frost, but not their interaction, constrain European beech and Silver fir growth in their southern distribution limits. Agric. For. Meteorol. 278, 107695. https://doi.org/10.1016/j.agrformet.2019.107695.

Gray, L.J., Beer, J., Geller, M., Haigh, J.D., Lockwood, M., Matthes, K., Cubasch, U., Fleitmann, D., Harrison, G., Hood, L., Luterbacher, J., Meehl, G.A., Shindell, D., Van Geel, B., White, W., 2010. Solar influences on climate. Rev. Geophys. 48, 2009RG000282. https://doi.org/10.1029/2009RG000282.

Gray, L.J., Woollings, T.J., Andrews, M., Knight, J., 2016. Eleven-year solar cycle signal in the NAO and Atlantic/European blocking. Q. J. R. Meteorol. Soc. 142, 1890–1903. https://doi.org/10.1002/qj.2782.

Hall, R., Erdélyi, R., Hanna, E., Jones, J.M., Scaife, A.A., 2015. Drivers of North Atlantic polar front jet stream variability. Int. J. Climatol. 35, 1697–1720. https://doi.org/10.1002/joc.4121.

Hathaway, D.H., 2015. The solar cycle. Living Rev. Sol. Phys. 12, 4. https://doi.org/10.1007/lrsp-2015-4.

Haywood, J., Boucher, O., 2000. Estimates of the direct and indirect radiative forcing due to tropospheric aerosols: a review. Rev. Geophys. 38, 513–543. https://doi.org/10.1029/1999RG000078.

Heinimann, H.R., 2010. A concept in adaptive ecosystem management-An engineering perspective. For. Ecol. Manag. 259, 848–856. https://doi.org/10.1016/j.foreco.2009.09.032.

Hernández-Almeida, I., Grosjean, M., Przybylak, R., Tylmann, W., 2015. A chrysophyte-based quantitative reconstruction of winter severity from varved lake sediments in NE Poland during the past millennium and its relationship to natural climate variability. Quat. Sci. Rev. 122, 74–88. https://doi.org/10.1016/j.quascirev.2015.05.029.

Hurrell, J.W., 1995. Decadal trends in the North atlantic oscillation: regional temperatures and precipitation. Science 269, 676–679. https://doi.org/10.1126/science.269.5224.676.

Iles, C., Hegerl, G., 2017. Role of the North atlantic oscillation in decadal temperature trends. Environ. Res. Lett. 12, 114010. https://doi.org/10.1088/1748-9326/aa9152.

Jarzyna, K., 2021. Climatic hazards for native tree species in Poland with special regards to silver fir (*Abies alba* Mill.) and European beech (*Fagus sylvatica* L.). Theor. Appl. Climatol. 144, 581–591. https://doi.org/10.1007/s00704-021-03550-y.

Jayaraman, A., Lubin, D., Ramachandran, S., Ramanathan, V., Woodbridge, E., Collins, W.D., Zalpuris, K.S., 1998. Direct observations of aerosol radiative forcing over the tropical Indian Ocean during the January-February 1996 pre-INDOEX cruise. J. Geophys. Res. 103, 13827–13836.

Johnson, J.T., Howitt, R., Cajete, G., Berkes, F., Louis, R.P., Kliskey, A., 2016. Weaving Indigenous and sustainability sciences to diversify our methods. Sustain. Sci. 11, 1–11. https://doi.org/10.1007/s11625-015-0349-x.

Jones, P.D., Jonsson, T., Wheeler, D., 1997. Extension to the North Atlantic Oscillation using early instrumental pressure observations from Gibraltar and south-west Iceland. Int. J. Climatol. 17, 1433–1450. https://doi.org/10.1002/(sici)1097-0088(19971115)17:13<1433::aid-joc203>3.3.co;2-g.

Kasatkina, E.A., Shumilov, O.I., Timonen, M., 2019. Solar activity imprints in tree ring-data from northwestern Russia. J. Atmos. Sol. Terr. Phys. 193, 105075. https://doi.org/10.1016/j.jastp.2019.105075.

Kelebek, M.B., Batibeniz, F., Önol, B., 2021. Exposure assessment of climate extremes over the Europe–Mediterranean region. Atmosphere 12, 633. https://doi.org/10.3390/atmos12050633.

Kjellström, E., Thejll, P., Rummukainen, M., Christensen, J.H., Boberg, F., Christensen, O.B., Maule, C.F., 2013. Emerging regional climate change signals for Europe under varying large-scale circulation conditions. Clim. Res. 56, 103–119. https://doi.org/10.3354/cr01146.

Klopčič, M., Mina, M., Bugmann, H., Bončina, A., 2017. The prospects of silver fir (*Abies alba* Mill.) and Norway spruce (*Picea abies* (L.) Karst) in mixed mountain forests under various management strategies, climate change and high browsing pressure. Eur. J. For. Res. 136, 1071–1090. https://doi.org/10.1007/s10342-017-1052-5.

Kolář, T., Čermák, P., Oulehle, F., Trnka, M., Štěpánek, P., Cudlín, P., Hruška, J., Büntgen, U., Rybníček, M., 2015. Pollution control enhanced spruce growth in the "Black Triangle" near the Czech-Polish border. Sci. Total Environ. 538, 703–711. https://doi.org/10.1016/j.scitotenv.2015.08.105.

Komitov, B., 2021. The European beech annual tree ring widths time series, solar–climatic relationships and solar dynamo regime changes. Atmosphere 12, 829. https://doi.org/10.3390/atmos12070829.

Konnert, M., Bergmann, F., 1995. The geographical distribution of genetic variation of silver fir (*Abies alba, Pinaceae*) in relation to its migration history. Plant Syst. Evol. 196, 19–30. https://doi.org/10.1007/BF00985333.

Kopp, G., 2021. Greg Kopp's TSI Page. TSI Clim. Data Rec. https://spot.colorado.edu/%7ekoppg/TSI/. (Accessed 4 February 2021).

Kopp, G., Krivova, N., Wu, C.J., Lean, J., 2016. The impact of the revised sunspot record on solar irradiance reconstructions. Sol. Phys. 291, 2951–2965. https://doi.org/10.1007/s11207-016-0853-x.

Köppen, W., 1936. Das Geographische System der Klimate, Handbuch der Klimatologie. Gebrüder Borntraeger, Berlin.

Kraft, G., 1884. Beiträge zur lehre von den durchforstungen, schlagstellungen und lichtungshieben. Klindworth, Hannover, Germany.

Kučeravá, B., Dobrovolný, L., Remeš, J., 2013. Responses of *Abies alba* seedlings to different site conditions in *Picea abies* plantations. Dendrobiology 69, 49–58. https://doi.org/10.12657/denbio.069.006.

Larsson, L.A., 2013. Cybis Elektronik & Data AB. https://www.cybis.se/. (Accessed 20 June 2019).

Laurenz, L., Lüdecke, H.J., Lüning, S., 2019. Influence of solar activity changes on European rainfall. J. Atmos. Sol. Terr. Phys. 185, 29–42. https://doi.org/10.1016/j.jastp.2019.01.012.

Lean, J., Beer, J., Bradley, R., 1995. Reconstruction of solar irradiance since 1610: implications for climate change. Geophys. Res. Lett. 22, 3195–3198. https://doi.org/10.1029/95GL03093.

Lean, J., Rottman, G., Harder, J., Kopp, G., 2005. Change and solar variability. Sol. Phys. 230, 27–53.

Li, W., Yue, F., Wang, C., Liao, J., Zhang, X., 2022. Climatic influences on intra-annual stem variation of *Larix principis-rupprechtii* in a semi-arid region. Front. For. Glob. Chang. 5, 948022. https://doi.org/10.3389/ffgc.2022.948022.

Lebourgeois, F., Rathgeber, C.B.K., Ulrich, E., 2010. Sensitivity of French temperate coniferous forests to climate variability and extreme events (*Abies alba*, *Picea abies* and *Pinus sylvestris*). J. Veg. Sci. 21, 364–376. https://doi.org/10.1111/j.1654-1103.2009.01148.x.

Li, T., Liu, Y., Cai, Q., Duan, X., Li, P., Ren, M., Ye, Y., 2023. Water stress-induced divergence growth of *Picea schrenkiana* in the western Tianshan and its forcing mechanisms. Forests 14, 354. https://doi.org/10.3390/f14020354.

Ligges, U., Short, T., Kienzle, P., Schnackenberg, S., Billinghurst, D., Borchers, H.-W., Carezia, A., Dupuis, P., Eaton, J.W., Frahi, W., Habel, K., Hornik, K., Krey, S., Lash, B., Leisch, F., Mersmann, O., Neis, P., Ruohio, J., Smith, J.O., Stewart, D., Weingessel, A., 2015. Signal Processing. R Package Signal. https://cran.r-project.org/web/packages/signal/. (Accessed 10 November 2022).

Lüdecke, H.J., Cina, R., Dammschneider, H.J., Lüning, S., 2020. Decadal and multidecadal natural variability in European temperature. J. Atmos. Sol. Terr. Phys. 205, 105294. https://doi.org/10.1016/j.jastp.2020.105294.

Łuszczyńska, K., Wistuba, M., Malik, I., 2018. Reductions in tree-ring widths of silver fir (*Abies alba* Mill.) as an indicator of air pollution in southern Poland. Environ. Soc. Econ. Stud. 6, 44–51. https://doi.org/10.2478/environ-2018-0022.

Ma, H., Chen, H., Gray, L., Zhou, L., Li, X., Wang, R., Zhu, S., 2018. Changing response of the North Atlantic/European winter climate to the 11 year solar cycle. Environ. Res. 13, 034007. https://doi.org/10.1088/1748-9326/aa9e94.

Maghrabi, A., Kudela, K., 2019. Relationship between time series cosmic ray data and aerosol optical properties: 1999–2015. J. Atmos. Sol. Terr. Phys. 190, 36–44. https://doi.org/10.1016/j.jastp.2019.04.014.

Magri, D., 2008. Patterns of post-glacial spread and the extent of glacial refugia of European beech (*Fagus sylvatica*). J. Biogeogr. 35, 450–463. https://doi.org/10.1111/j.1365-2699.2007.01803.x.

Matveev, S.M., Chendev, Y.G., Lupo, A.R., Hubbart, J.A., Timashchuk, D.A., 2017. Climatic changes in the East-European forest-steppe and effects on Scots Pine productivity. Pure Appl. Geophys. 174, 427–443. https://doi.org/10.1007/s00024-016-1420-y.

Mauri, A., de Rigo, D., Caudullo, G., 2016. *Abies alba* in Europe: distribution, habitat, usage and threats. In: San-Miguel-Ayanz, J., de Rigo, D., Caudullo, G., Durrant, T.H., Mauri, A. (Eds.), European Atlas of Forest Tree Species. Publications Office of the European Union, Luxembourg, p. 1493.

Maxime, C., Hendrik, D., 2011. Effects of climate on diameter growth of co-occurring *Fagus sylvatica* and *Abies alba* along an altitudinal gradient. Trees (Berl.) 25, 265–276. https://doi.org/10.1007/s00468-010-0503-0.

Mihai, G., Alexandru, A.M., Stoica, E., Birsan, M.V., 2021. Intraspecific growth response to drought of *Abies alba* in the southeastern Carpathians. Forests 12, 387. https://doi.org/10.3390/f12040387.

Mikulenka, P., Prokůpková, A., Vacek, Z., Vacek, S., Bulušek, D., Simon, J., Šimůnek, V., Hájek, V., 2020. Effect of climate and air pollution on radial growth of mixed forests: *Abies alba* Mill. vs. *Picea abies* (L.) Karst. Cent. Eur. For. J. 66, 23–36. https://doi.org/10.2478/forj-2019-0026.

Milad, M., Schaich, H., Bürgi, M., Konold, W., 2011. Climate change and nature conservation in Central European forests: a review of consequences, concepts and challenges. For. Ecol. Manag. 261, 829–843. https://doi.org/10.1016/j.foreco.2010.10.038.

Muraki, Y., Masuda, K., Nagaya, K., Wada, K., Miyahara, H., 2011. Solar variability and width of tree ring. Astrophys. Space Sci. Trans. 7, 395–401. https://doi.org/10.5194/astra-7-395-2011.

Naumann, G., Cammalleri, C., Mentaschi, L., Feyen, L., 2021. Increased economic drought impacts in Europe with anthropogenic warming. Nat. Clim. Chang. 11, 485–491. https://doi.org/10.1038/s41558-021-01044-3.

Nussbaumer, A., Meusburger, K., Schmitt, M., Waldner, P., Gehrig, R., Haeni, M., Rigling, A., Brunner, I., Thimonier, A., 2020. Extreme summer heat and drought lead to early fruit abortion in European beech. Sci. Rep. 10, 5334. https://doi.org/10.1038/s41598-020-62073-0.

Ols, C., Trouet, V., Girardin, M.P., Hofgaard, A., Bergeron, Y., Drobyshev, I., 2018. Post-1980 shifts in the sensitivity of boreal tree growth to North Atlantic Ocean dynamics and seasonal climate. Glob. Planet. Chang. 165, 1–12. https://doi.org/10.1016/j.gloplacha.2018.03.006.

Ormes, J.F., 2018. Cosmic rays and climate. Adv. Space Res. 62, 2880–2891. https://doi.org/10.1016/j.asr.2017.07.028.

Ossó, A., Allan, R.P., Hawkins, E., Shaffrey, L., Maraun, D., 2022. Emerging new climate extremes over Europe. Clim. Dynam. 58, 487–501. https://doi.org/10.1007/s00382-021-05917-3.

PCRB, 2022. Protezione Civile – Regione Basilicata. http://www.centrofunzionalebasilicata.it/it/. (Accessed 10 November 2022).

Pinto, P.E., Gégout, J.C., Hervé, J.C., Dhôte, J.F., 2008. Respective importance of ecological conditions and stand composition on *Abies alba* Mill. Dominant height growth. For. Ecol. Manag. 255, 619–629. https://doi.org/10.1016/j.foreco.2007.09.031.

Piovesan, G., Biondi, F., Di Filippo, A., Alessandrini, A., Maugeri, M., 2008. Drought-driven growth reduction in old beech (*Fagus sylvatica* L.) forests of the central Apennines, Italy. Glob. Chang. Biol. 14, 1265–1281. https://doi.org/10.1111/j.1365-2486.2008.01570.x.

Podrázský, V., Vacek, Z., Kupka, I., Vacek, S., Třeštík, M., Cukor, J., 2018. Effects of silver fir (*Abies alba* Mill.) on the humus forms in Norway spruce (*Picea abies* (L.) H. Karst.) stands. J. For. Sci. 64, 245–250. https://doi.org/10.17221/19/2018-JFS.

Ponocná, T., Chuman, T., Rydval, M., Urban, G., Migała, K., Treml, V., 2018. Deviations of treeline Norway spruce radial growth from summer temperatures in East-Central Europe. Agric. For. Meteorol. 253–254, 62–70. https://doi.org/10.1016/j.agrformet.2018.02.001.

Putalová, T., Vacek, Z., Vacek, S., Štefančík, I., Bulušek, D., Král, J., 2019. Tree-ring widths as an indicator of air pollution stress and climate conditions in different Norway spruce forest stands in the Krkonoše Mts. Cent. Eur. For. J. 65, 21–33. https://doi.org/10.2478/forj-2019-0004.

Remeš, J., Bílek, L., Novák, J., Vacek, Z., Vacek, S., Putalová, T., Koubek, L., 2015. Diameter increment of beech in relation to social position of trees, climate characteristics and thinning intensity. J. For. Sci. 61, 456–464. https://doi.org/10.17221/75/2015-JFS.

Rinntech, 2010. TSAP-WIN: Time series analysis and presentation for dendrochronology and related applications. Heidelberg, Germany.

Royal Observatory of Belgium, 2023. Total Solar Irradiance -Royal Observatory of Belgium, Solar Influences Data Analysis Center. https://www.sidc.be/observations/space-based-timelines/tsi. (Accessed 7 November 2023).

Ruosch, M., Spahni, R., Joos, F., Henne, P.D., van der Knaap, W.O., Tinner, W., 2016. Past and future evolution of *Abies alba* forests in Europe–comparison of a dynamic vegetation model with palaeo data and observations. Glob. Chang. Biol. 22, 727–740. https://doi.org/10.1111/gcb.13075.

Saffioti, C., Fischer, E.M., Scherrer, S.C., Knutti, R., 2016. Reconciling observed and modeled temperature and precipitation trends over Europe by adjusting for circulation variability. Geophys. Res. Lett. 43, 8189–8198. https://doi.org/10.1002/2016GL069802.

Shumilov, O.I., Kasatkina, E.A., Mielikainen, K., Timonen, M., Kanatjev, A.G., 2011. Palaeovolcanos, Solar activity and pine tree-rings from the Kola Peninsula (northwestern Russia) over the last 560 years. Int. J. Environ. Res. 5, 855–864.

Šimůnek, V., Vacek, Z., Vacek, S., Králíček, I., Vančura, K., 2019. Growth variability of European beech (*Fagus sylvatica* L.) natural forests: dendroclimatic study from Krkonoše National Park. Cent. Eur. For. J. 65, 92–102. https://doi.org/10.2478/forj-2019-0010.

Šimůnek, V., Sharma, R.P., Vacek, Z., Vacek, S., Hůnová, I., 2020a. Sunspot area as unexplored trend inside radial growth of European beech in Krkonoše Mountains : a forest science from different perspective. Eur. J. For. Res. 139, 999–1013. https://doi.org/10.1007/s10342-020-01302-7.

Šimůnek, V., Vacek, Z., Vacek, S., 2020b. Solar cycles in salvage logging: national data from the Czech Republic confirm significant correlation. Forests 11, 973. https://doi.org/10.3390/f11090973.

Šimůnek, V., Vacek, S., Vacek, Z., Andrea, G.D., 2021a. Vztahy těžby listnatých a jehličnatých dřevin dle slunečních cyklů (enl: harvesting fluctuations of deciduous and coniferous tree species according to solar cycles). In: Houšková, K., Jan, D. (Eds.), Proceedings of Central European Silviculture–21st International Conference. Mendel University in Brno, The Czeck Republic, pp. 101–108.

Šimůnek, V., Vacek, Z., Vacek, S., Ripullone, F., Hájek, V., D'Andrea, G., 2021b. Tree rings of european beech (*Fagus sylvatica* l.) indicate the relationship with solar cycles during climate change in central and southern europe. Forests 12, 259. https://doi.org/10.3390/f12030259.

Singh, A.K., Bhargawa, A., 2020. Delineation of possible influence of solar variability and galactic cosmic rays on terrestrial climate parameters. Adv. Space Res. 65, 1831–1842. https://doi.org/10.1016/j.asr.2020.01.006.

Slanař, J., Vacek, Z., Vacek, S., Bulušek, D., Cukor, J., Štefančík, I., Bílek, L., Král, J., 2017. Long-term transformation of submontane spruce-beech forests in the Jizerské hory Mts.: dynamics of natural regeneration. Cent. Eur. For. J. 63, 212–224. https://doi.org/10.1515/forj-2017-0023.

Šmilauer, P., Lepš, J., 2014. Multivariate Analysis of Ecological Data Using CANOCO 5. Cambridge University Press, New York.

Smith, D.M., Eade, R., Scaife, A.A., Caron, L.-P., Danabasoglu, G., DelSole, T.M., Delworth, T., Doblas-Reyes, F.J., Dunstone, N.J., Hermanson, L., Kharin, V., Kimoto, M., Merryfield, W.J., Mochizuki, T., Müller, W.A., Pohlmann, H., Yeager, S., Yang, X., 2019. Robust skill of decadal climate predictions. npj Clim. Atmos. Sci. 2, 13. https://doi.org/10.1038/s41612-019-0071-y.

Smith, D.M., Scaife, A.A., Eade, R., Athanasiadis, P., Bellucci, A., Bethke, I., Bilbao, R., Borchert, L.F., Caron, L.-P., Counillon, F., Danabasoglu, G., Delworth, T., Doblas-Reyes, F.J., Dunstone, N.J., Estella-Perez, V., Flavoni, S., Hermanson, L., Keenlyside, N., Kharin, V., Kimoto, M., Merryfield, W.J., Mignot, J., Mochizuki, T., Modali, K., Monerie, P.-A., Müller, W.A., Nicolí, D., Ortega, P., Pankatz, K., Pohlmann, H., Robson, J., Ruggieri, P., Sospedra-Alfonso, R., Swingedouw, D., Wang, Y., Wild, S., Yeager, S., Yang, X., Zhang, L., 2020. North Atlantic climate far more predictable than models imply. Nature 583, 796–800.

Speer, J.H., 2010. Fundamentals of Tree-Ring Research. University of Arizona Press, Tuscon.

St George, S., 2014. An overview of tree-ring width records across the Northern Hemisphere. Quat. Sci. Rev. 95, 132–150. https://doi.org/10.1016/j.quascirev.2014.04.029.

Stagge, J.H., Kingston, D.G., Tallaksen, L.M., Hannah, D.M., 2017. Observed drought indices show increasing divergence across Europe. Sci. Rep. 7, 1–10. https://doi.org/10.1038/s41598-017-14283-2.

StatSoft, 2013. Statistica Electronic Manual. https://www.scribd.com/document/321061529/STATISTICA-Electronic-Manual. (Accessed 7 November 2023).

Štefančík, I., Bošela, M., Petráš, R., 2018. Effect of different management on quality and value production of pure beech stands in Slovakia. Cent. Eur. For. J. 64, 24–32. https://doi.org/10.1515/forj-2017-0012.

Steirou, E., Gerlitz, L., Apel, H., Merz, B., 2017. Links between large-scale circulation patterns and streamflow in Central Europe: a review. J. Hydrol. 549, 484–500. https://doi.org/10.1016/j.jhydrol.2017.04.003.

Surový, P., Ribeiro, N.A., Pereira, J.S., Dorotovič, I., 2008. Influence of solar activity cycles on cork growth – a hypothesis. In: Dorotovič, I. (Ed.), Proc. Of the 19th National Solar Physics Meeting. Hurbanovo, SÚH, Papradno, pp. 67–72.

Tatli, H., Menteş, Ş.S., 2019. Detrended cross-correlation patterns between North Atlantic oscillation and precipitation. Theor. Appl. Climatol. 138, 387–397. https://doi.org/10.1007/s00704-019-02827-7.

Team R Core, 2022. A Language and Environment for Statistical Computing. R Foundation for Statistical Computing, Vienna, Austria.

Teodosiu, M., Mihai, G., Fussi, B., Ciocîrlan, E., 2019. Genetic diversity and structure of silver fir (*Abies alba* Mill.) at the south-eastern limit of its distribution range. Ann. For. Res. 62, 139–156. https://doi.org/10.15287/afr.2019.1436.

Tinner, W., Lotter, A.F., 2006. Holocene expansions of *Fagus silvatica* and *Abies alba* in Central Europe: where are we after eight decades of debate? Quat. Sci. Rev. 25, 526–549. https://doi.org/10.1016/j.quascirev.2005.03.017.

Tsanis, I., Tapoglou, E., 2019. Winter North Atlantic Oscillation impact on European precipitation and drought under climate change. Theor. Appl. Climatol. 135, 323–330. https://doi.org/10.1007/s00704-018-2379-7.

Tsiropoula, G., 2003. Signatures of solar activity variability in meteorological parameters. J. Atmos. Sol. Terr. Phys. 65, 469–482. https://doi.org/10.1016/S1364-6826(02)00295-X.

Tumajer, J., Altman, J., Štěpánek, P., Treml, V., Doležal, J., Cienciala, E., 2017. Increasing moisture limitation of Norway spruce in Central Europe revealed by forward modelling of tree growth in tree-ring network. Agric. For. Meteorol. 247, 56–64. https://doi.org/10.1016/j.agrformet.2017.07.015.

Vacek, Z., 2017. Structure and dynamics of spruce-beech-fir forests in Nature Reserves of the Orlické hory Mts. in relation to ungulate game. Cent. Eur. For. J. 63, 23–34. https://doi.org/10.1515/forj-2017-0006.

Vacek, Z., Vacek, S., Cukor, J., 2023. European forests under global climate change: review of tree growth processes, crises and management strategies. J. Environ. Manag. 332, 117353. https://doi.org/10.1016/j.jenvman.2023.117353.

Vicente-Serrano, S.M., López-Moreno, J.I., Lorenzo-Lacruz, J., Kenawy, A.E., Azorin-Molina, C., Morán-Tejeda, E., Pasho, E., Zabalza, J., Beguería, S., Angulo-Martínez, M., 2011. The NAO impact on droughts in the mediterranean region. In: Vicente-Serrano, S.M., Trigo, R.M. (Eds.), Hydrological, Socioeconomic and Ecological Impacts of the North Atlantic Oscillation in the Mediterranean Region. Springer Netherlands, Dordrecht, pp. 23–40.

Vicente-Serrano, S.M., García-Herrera, R., Barriopedro, D., Azorin-Molina, C., López-Moreno, J.I., Martín-Hernández, N., Tomás-Burguera, M., Gimeno, L., Nieto, R., 2016. The Westerly Index as complementary indicator of the North Atlantic oscillation in explaining drought variability across Europe. Clim. Dynam. 47, 845–863. https://doi.org/10.1007/s00382-015-2875-8.

Vitali, V., Büntgen, U., Bauhus, J., 2017. Silver fir and Douglas fir are more tolerant to extreme droughts than Norway spruce in south-western Germany. Glob. Chang. Biol. 23, 5108–5119. https://doi.org/10.1111/gcb.13774.

Vitasse, Y., Bottero, A., Rebetez, M., Conedera, M., Augustin, S., Brang, P., Tinner, W., 2019. What is the potential of silver fir to thrive under warmer and drier climate? Eur. J. For. Res. 138, 547–560. https://doi.org/10.1007/s10342-019-01192-4.

Volařík, D., Hédl, R., 2013. Expansion to abandoned agricultural land forms an integral part of silver fir dynamics. For. Ecol. Manag. 292, 39–48. https://doi.org/10.1016/j.foreco.2012.12.016.

Walder, D., Krebs, P., Bugmann, H., Manetti, M.C., Pollastrini, M., Anzillotti, S., Conedera, M., 2021. Silver fir (*Abies alba* Mill.) is able to thrive and prosper under meso-Mediterranean conditions. For. Ecol. Manag. 498, 119537. https://doi.org/10.1016/j.foreco.2021.119537.

Wang, Y.-M., Lean, J.L., Sheeley Jr., N.R., 2005. Modeling the Sun's magnetic field and irradiance since 1713. Astrophys. J. 625, 522–538. https://doi.org/10.1086/429689.

Wigley, T.M.L., Briffa, K.R., Jones, P.D., 1984. On the average value of correlated time series with applications in dendroclimatology and hydrometeorology. J. Clim. Appl. Meteorol. 23, 201–213.

Woods, T.N., Harder, J.W., Kopp, G., Snow, M., 2022. Solar-cycle variability results from the solar radiation and climate experiment (SORCE) mission. Sol. Phys. 297, 43. https://doi.org/10.1007/s11207-022-01980-z.

Yao, Y., Luo, D.H., 2014. Relationship between zonal position of the North Atlantic Oscillation and Euro-Atlantic blocking events and its possible effect on the weather over Europe. Sci. China Earth Sci. 57, 2628–2636. https://doi.org/10.1007/s11430-014-4949-6.

Zhang, Y., Guo, M., Wang, X., Gu, F., Liu, S., 2018. Divergent tree growth response to recent climate warming of *Abies faxoniana* at alpine treelines in east edge of Tibetan Plateau. Ecol. Res. 33, 303–311. https://doi.org/10.1007/s11284-017-1538-0.